

Simulação computacional da RAA em estruturas de concreto

**Eduardo M. R. Fairbairn, Marcos M. Silvos, Romildo D. Toledo Filho,
Fernando L. B. Ribeiro,**

COPPE/UFRJ

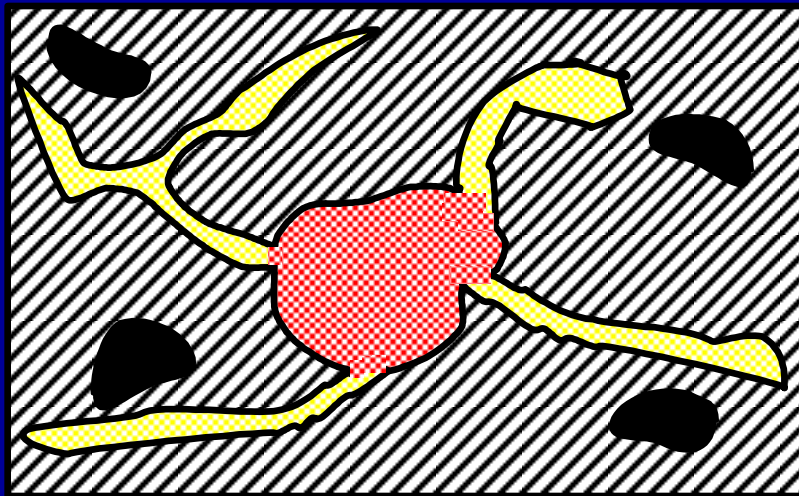
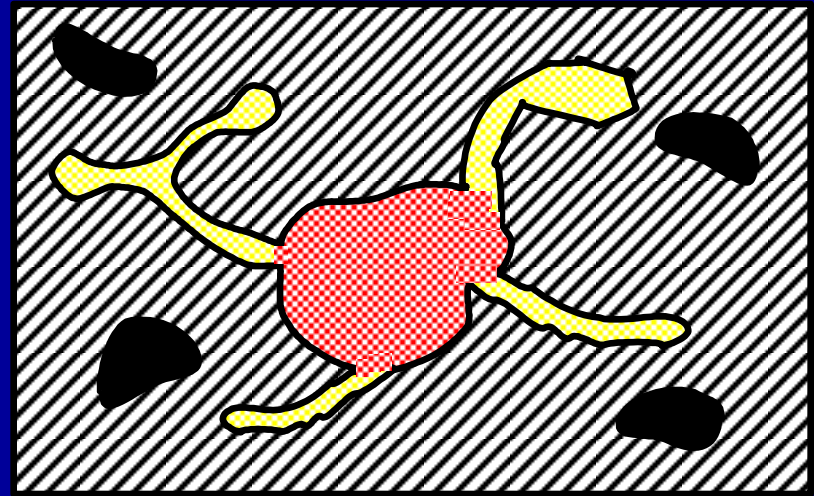
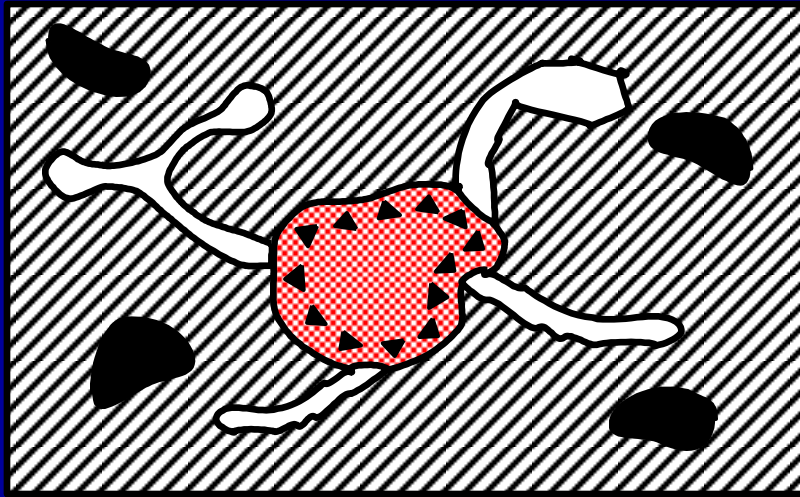







**Márcia F. F. Aguas
FURNAS CENTRAIS ELÉTRICAS S.A.**

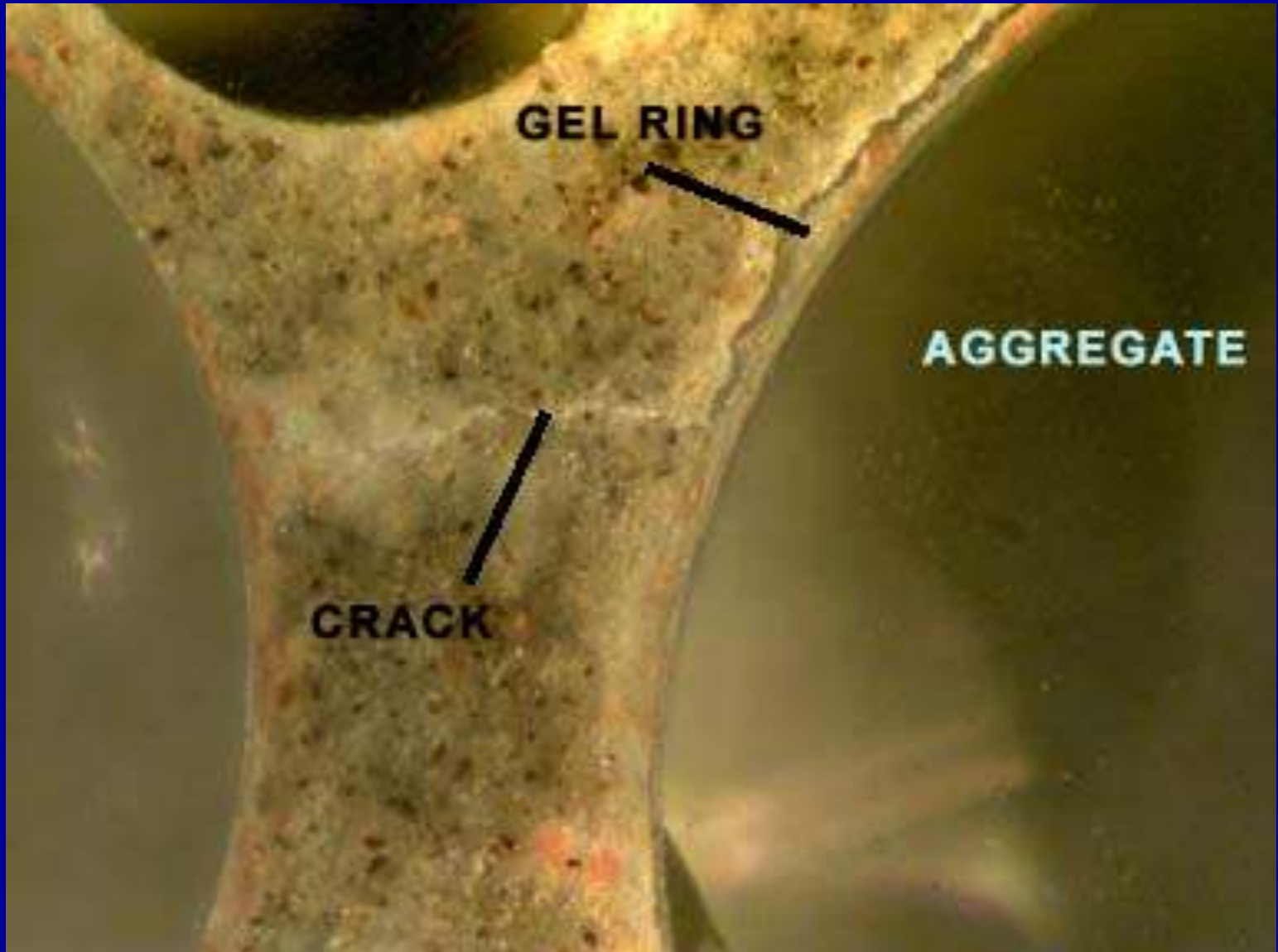


Physical principles of the model

(Glasser and Kataoka mechanism)

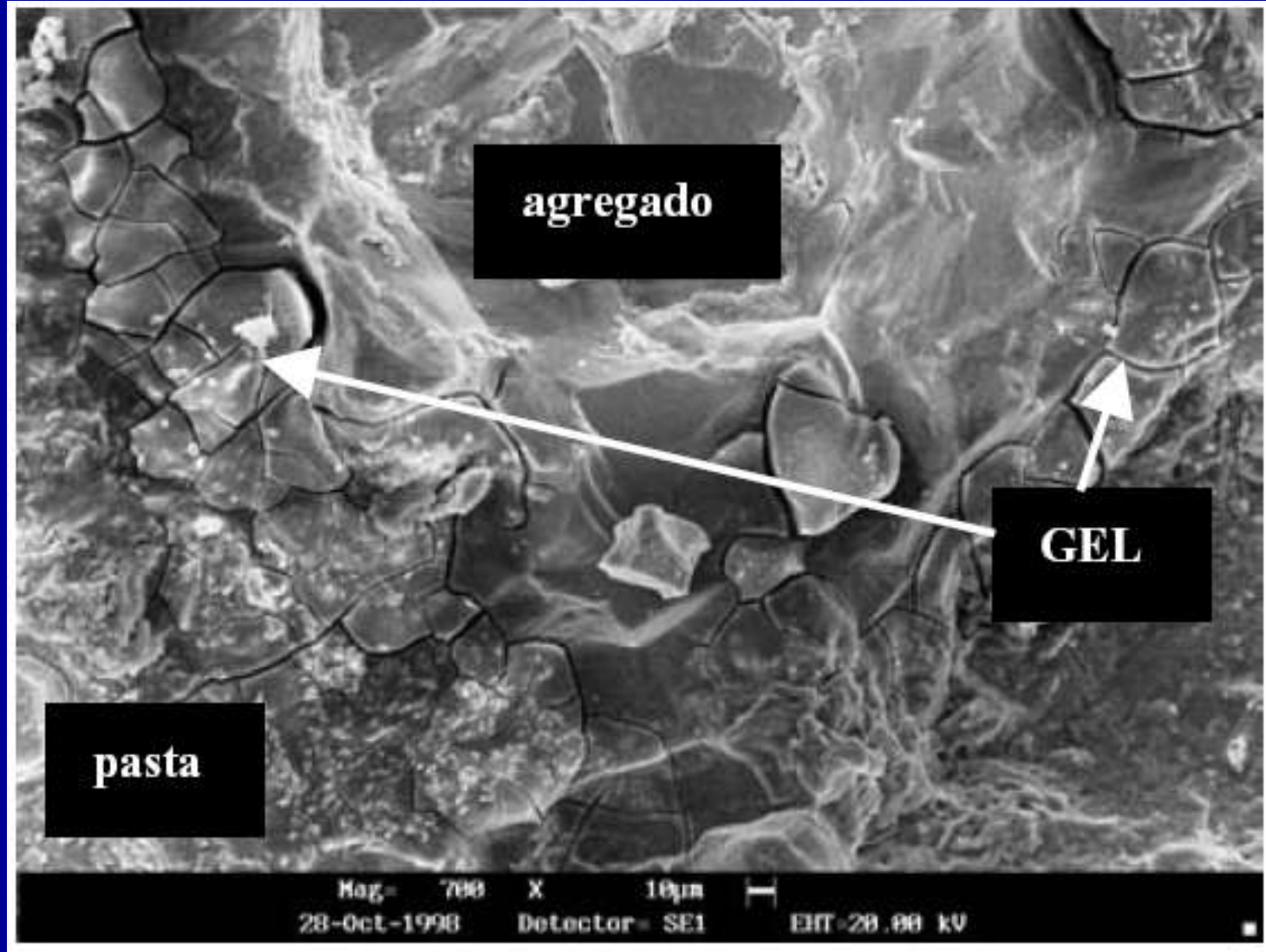


-  Reactive aggregate
-  Inert aggregate
-  Cement matrix
-  Pore
-  Pore + gel
(eventual crack)



Courtney Collins . Jason Ideker . Gayle Willis . Jessica Hurst, Virginia Tech

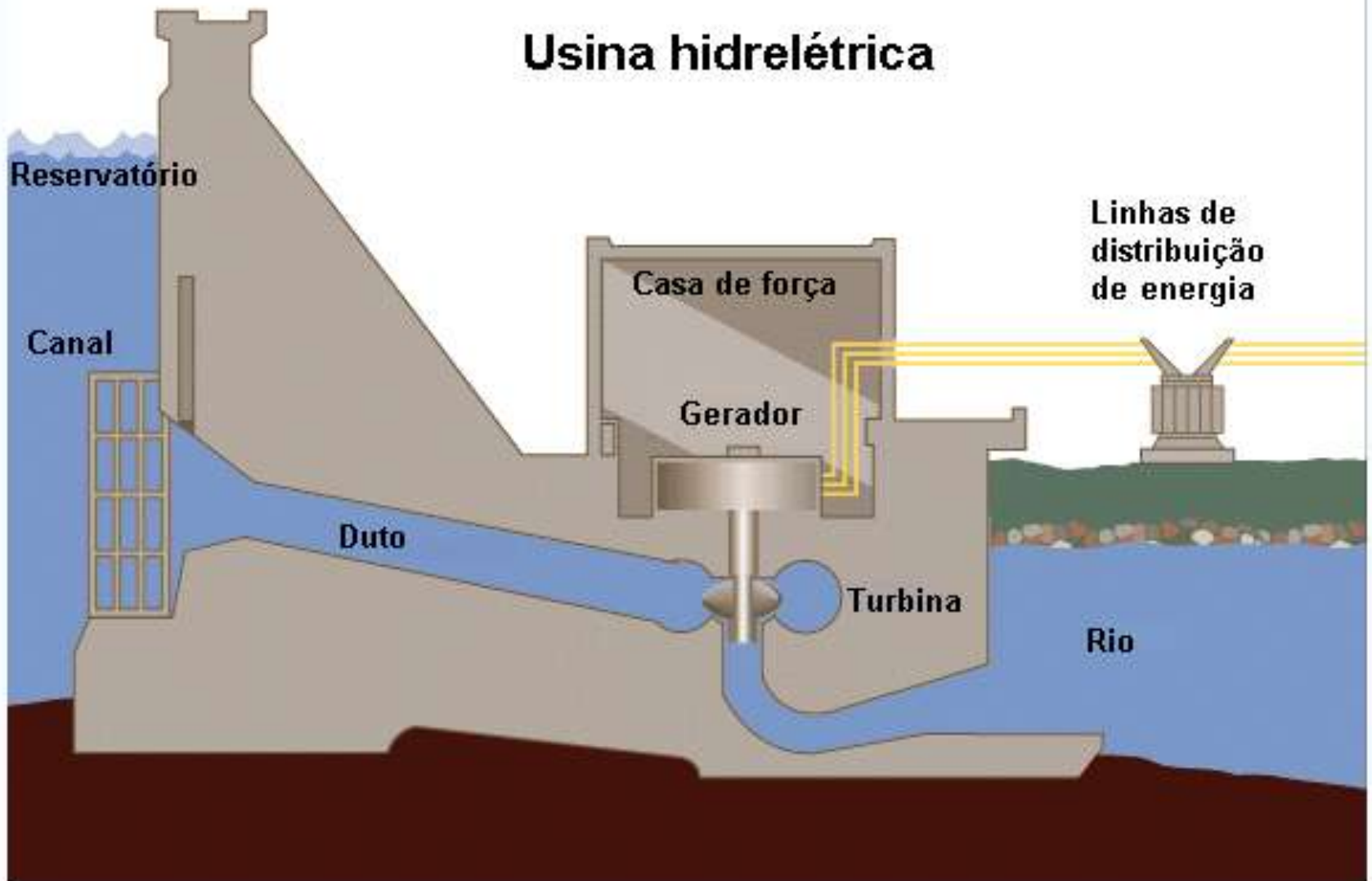
Physical principles of the model



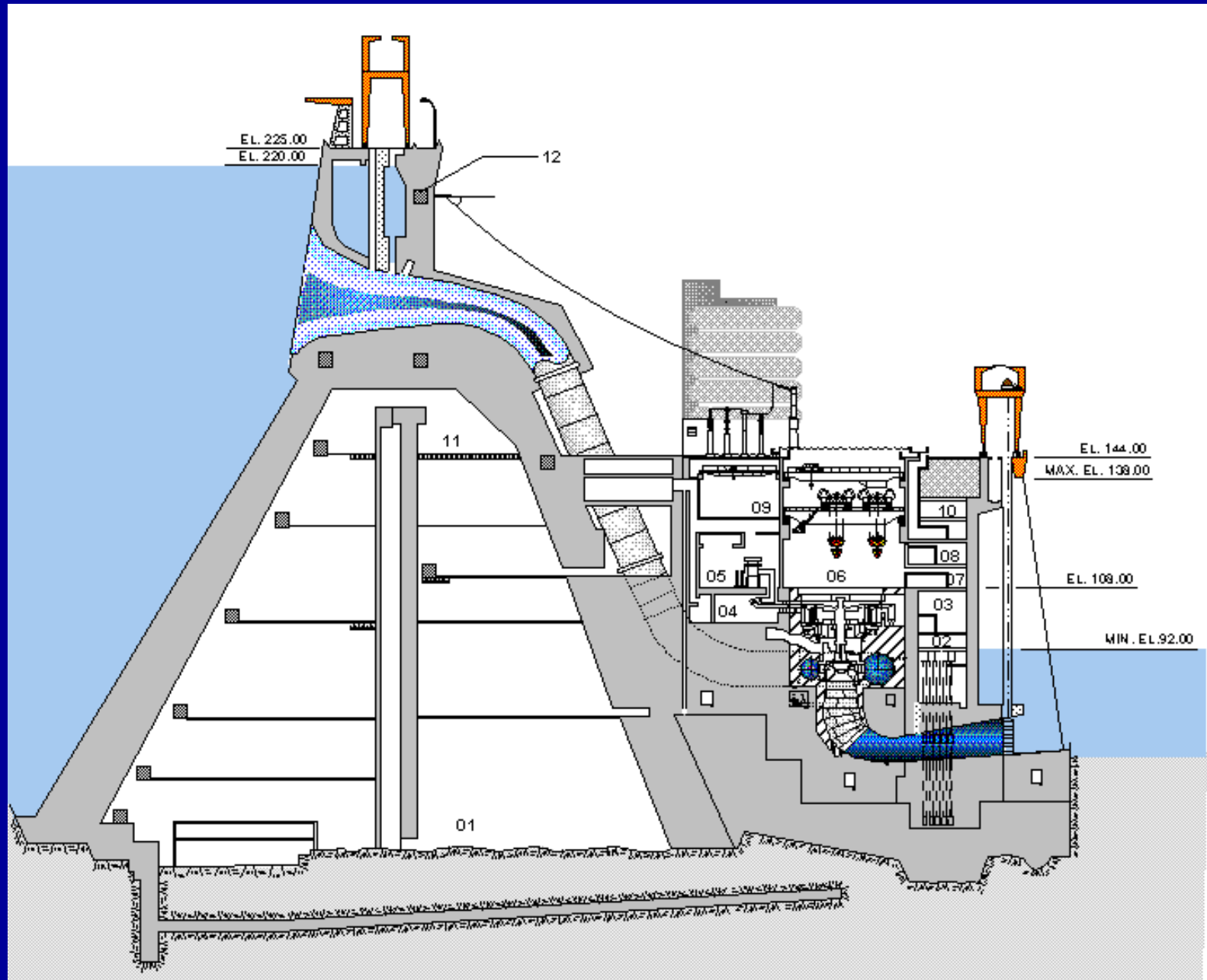
Physical principles of the model



Problems in an hydropower plant



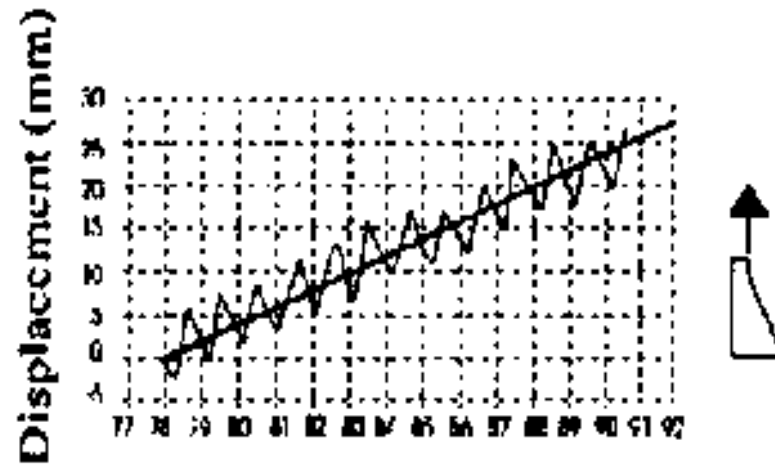
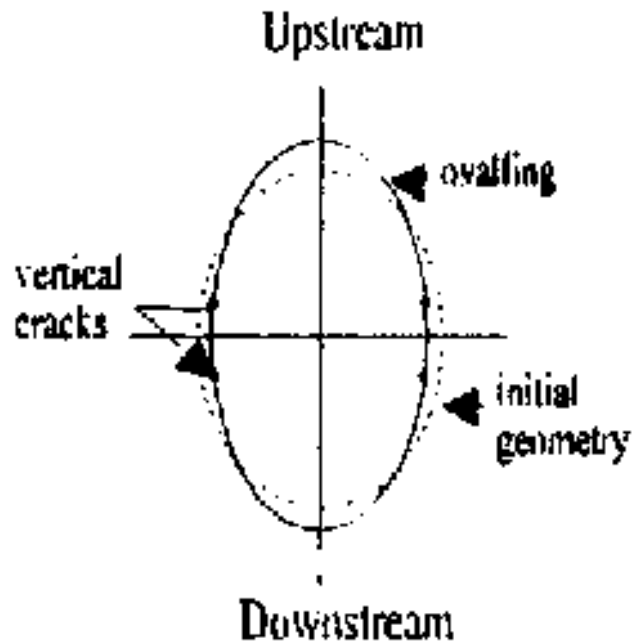
Problems in an hydropower plant



Problems in an hydropower plant

Beauharnois, Canada

Ovalling distortions of the pedestral throat ring. Elevation at the crest of about 2 mm/a.

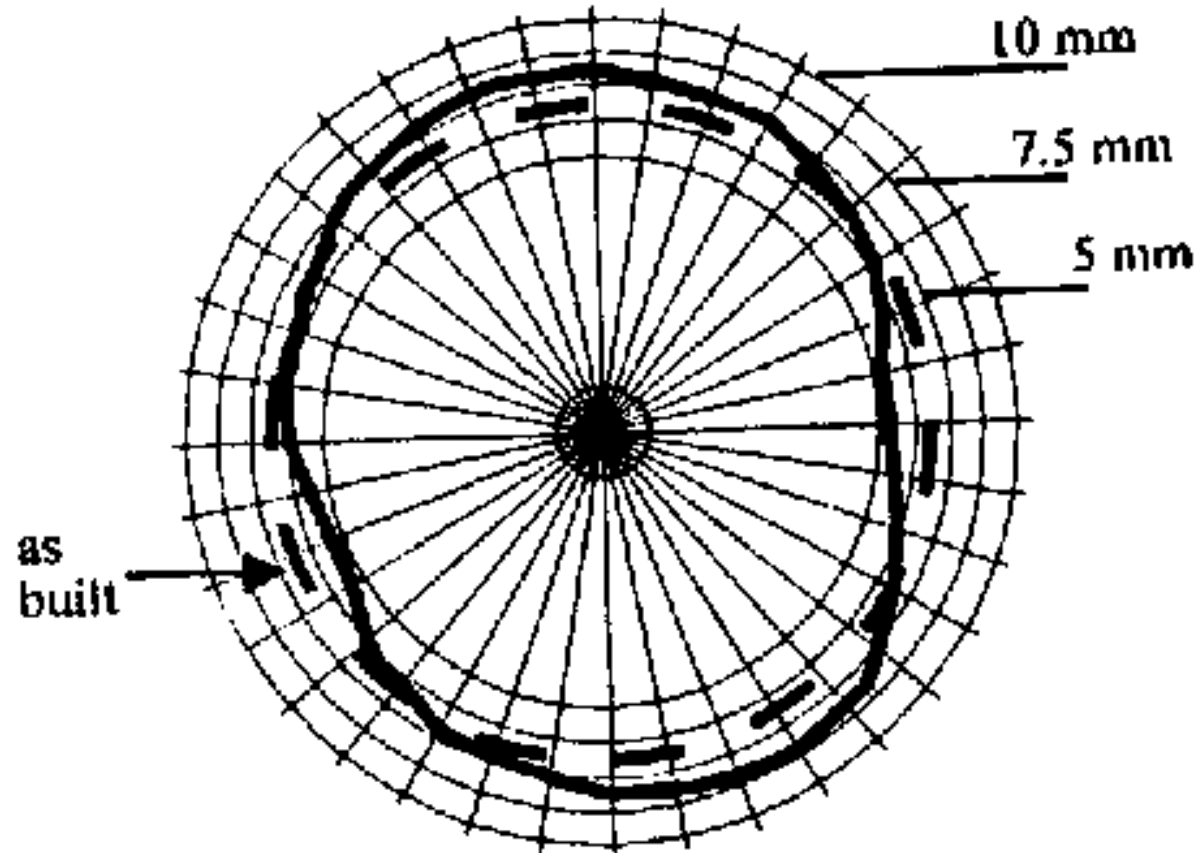


Deformation Time History

Problems in an hydropower plant

Mactaquac, Canada

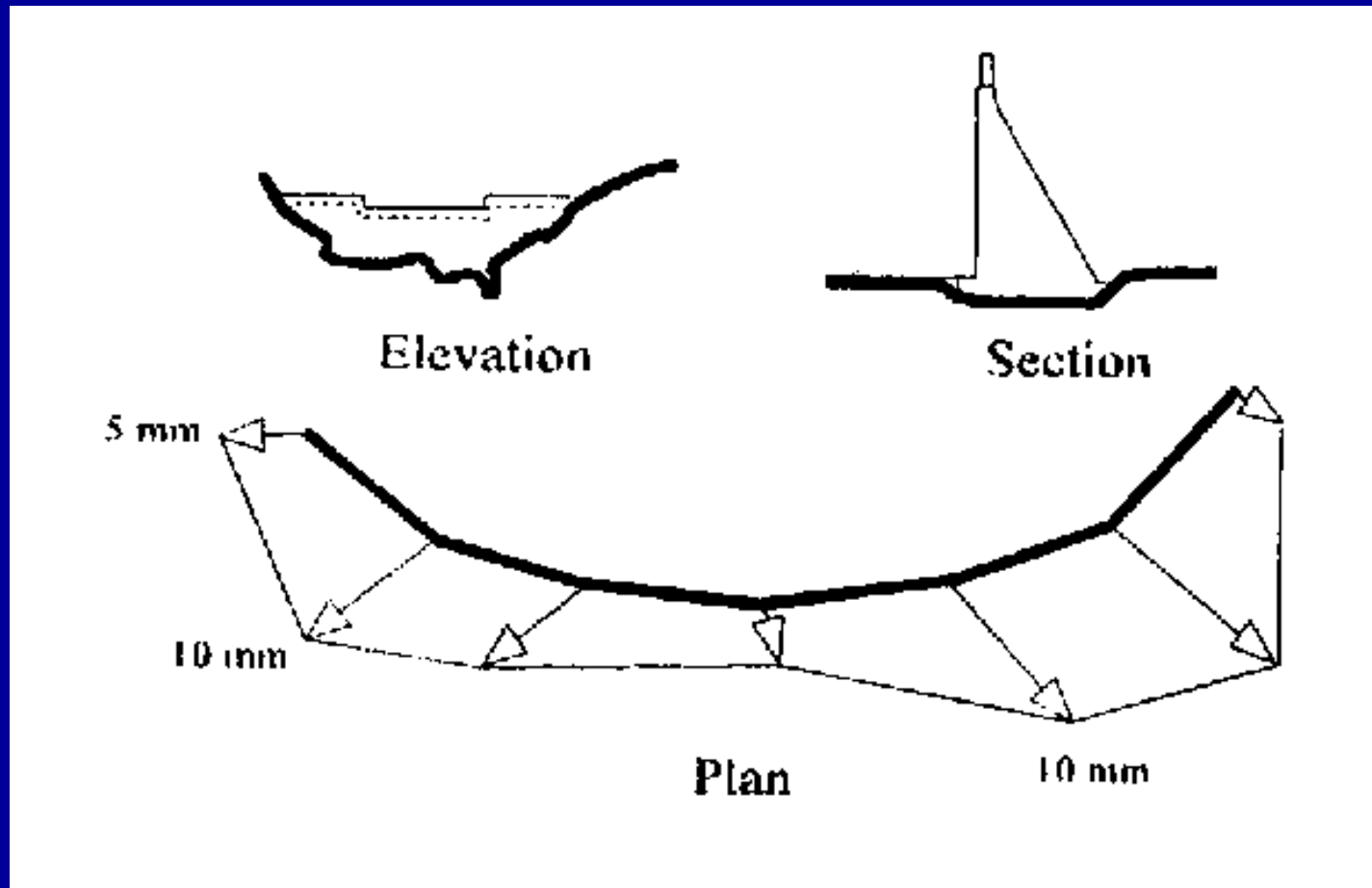
Discharge ring ovalization and corresponding reductions in turbine blade clearances.



Problems in an hydropower plant

Poortjieskloof, South Africa

Permanent upstream movement up to 20 mm over a period of 15 years and upward movement of about 2 mm over a period of 2 years.



Problems in an hydropower plant

Kumburu spillway, Kenya

Maximum crack width: 20 mm.

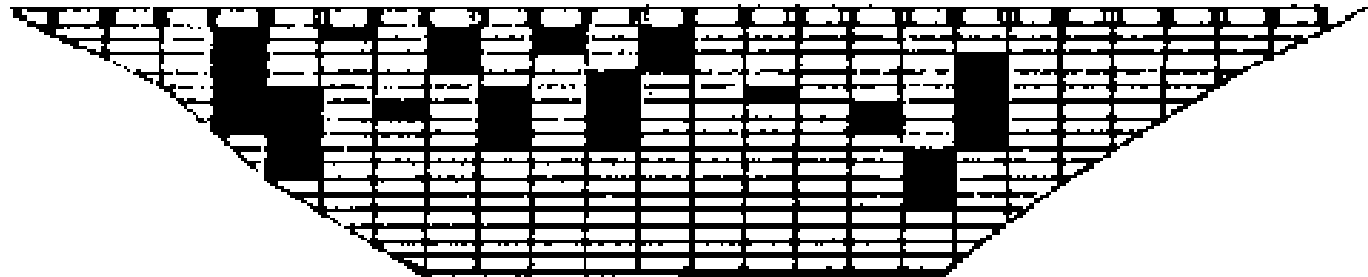
Piers distorted. Maximum deviation from vertical: 40 mm.



Problems in an hydropower plant

Val de la Mare, Jersey (United Kingdom)

Cracking and reduction in sonic velocities.



0.5 - 1 mm 1.5 - 2.5 mm 3 - 4 mm

Bases of the model

(some experimental evidences)

- AAR occurs if the structure is in contact with water.
 - The reaction is thermo-activated.
- The extension of the reaction is independent on stress levels ranging from 0 to 10 MPa .
- There is an anisotropy induced by the stress fields.



Pergamon

Available online at www.sciencedirect.com



Cement and Concrete Research 34 (2004) 492–505

**CEMENT AND
CONCRETE
RESEARCH**

Macroscopic model of concrete subjected to alkali–aggregate reaction

M.C.R. Farage*, J.L.D. Alves, E.M.R. Fairbairn

COMMUNICATIONS IN NUMERICAL METHODS IN ENGINEERING

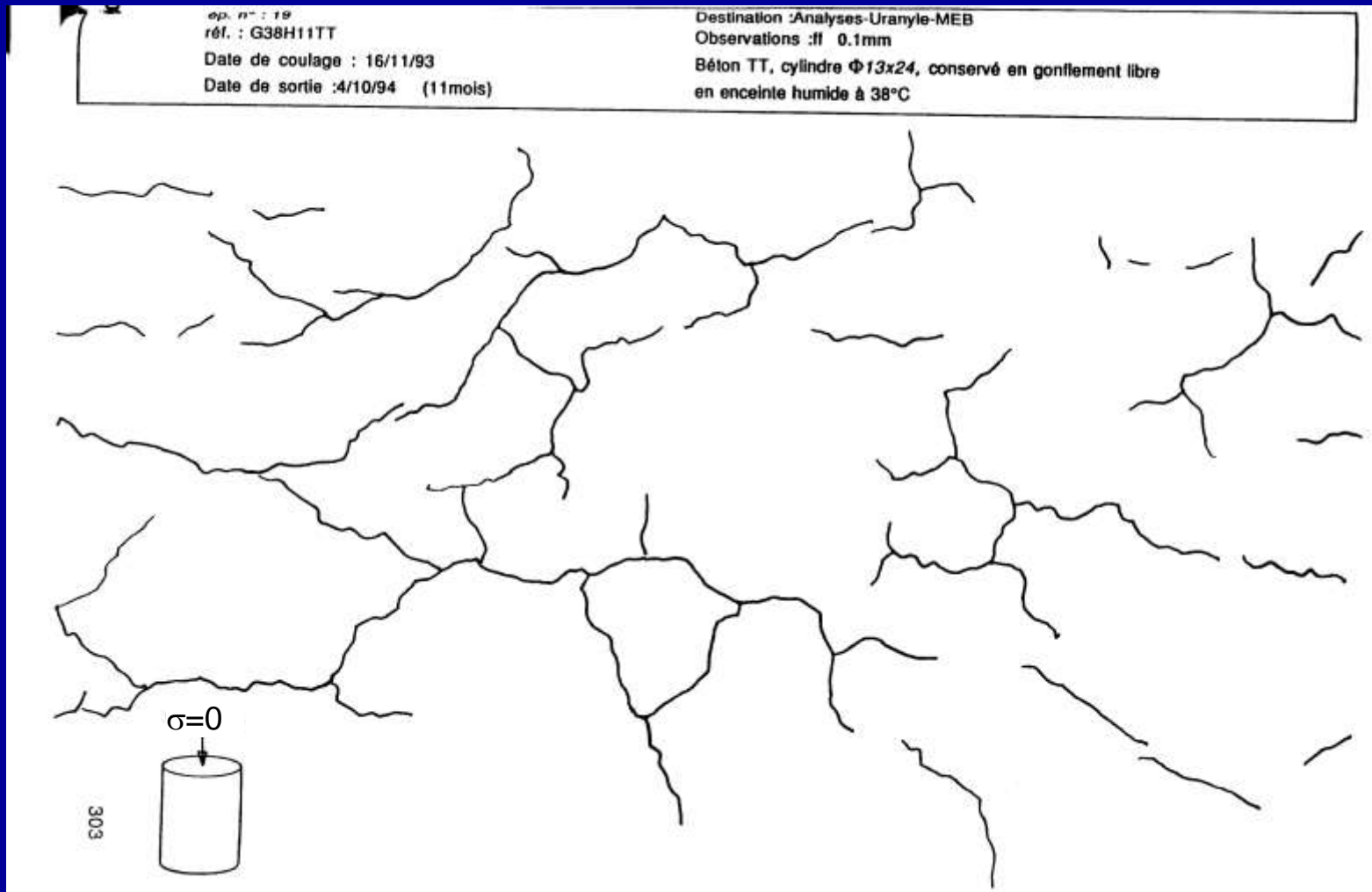
Commun. Numer. Meth. Engng (in press)

Published online in Wiley InterScience (www.interscience.wiley.com). DOI: 10.1002/cnm.788

Modelling the structural behaviour of a dam affected
by alkali–silica reaction

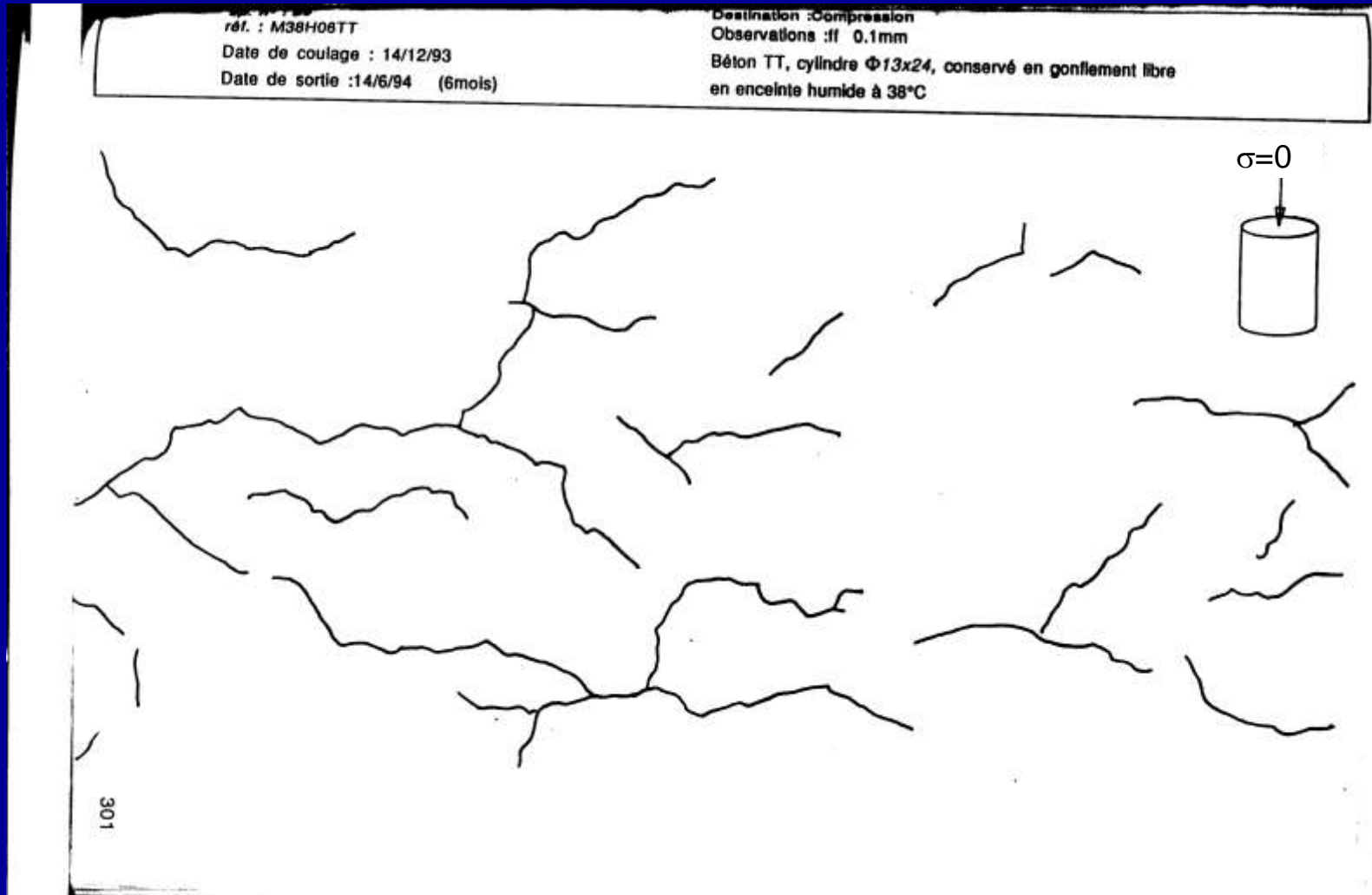
Eduardo M. R. Fairbairn*[†], Fernando L. B. Ribeiro, Luciana E. Lopes,
Romildo D. Toledo-Filho and Marcos M. Silvano

Cracking – free expansion – LCPC tests



(Larive, C., Apports combinés de l'alkali-réaction et de ses effets mécaniques, thèse de doctorat, E.N.P.C., Paris, France, 1997.)

Cracking – free expansion - LCPC tests



(Larive, C., Apports combinés de l'alkali-réaction et de ses effets mécaniques, thèse de doctorat, E.N.P.C., Paris, France, 1997.)

Cracking – free expansion



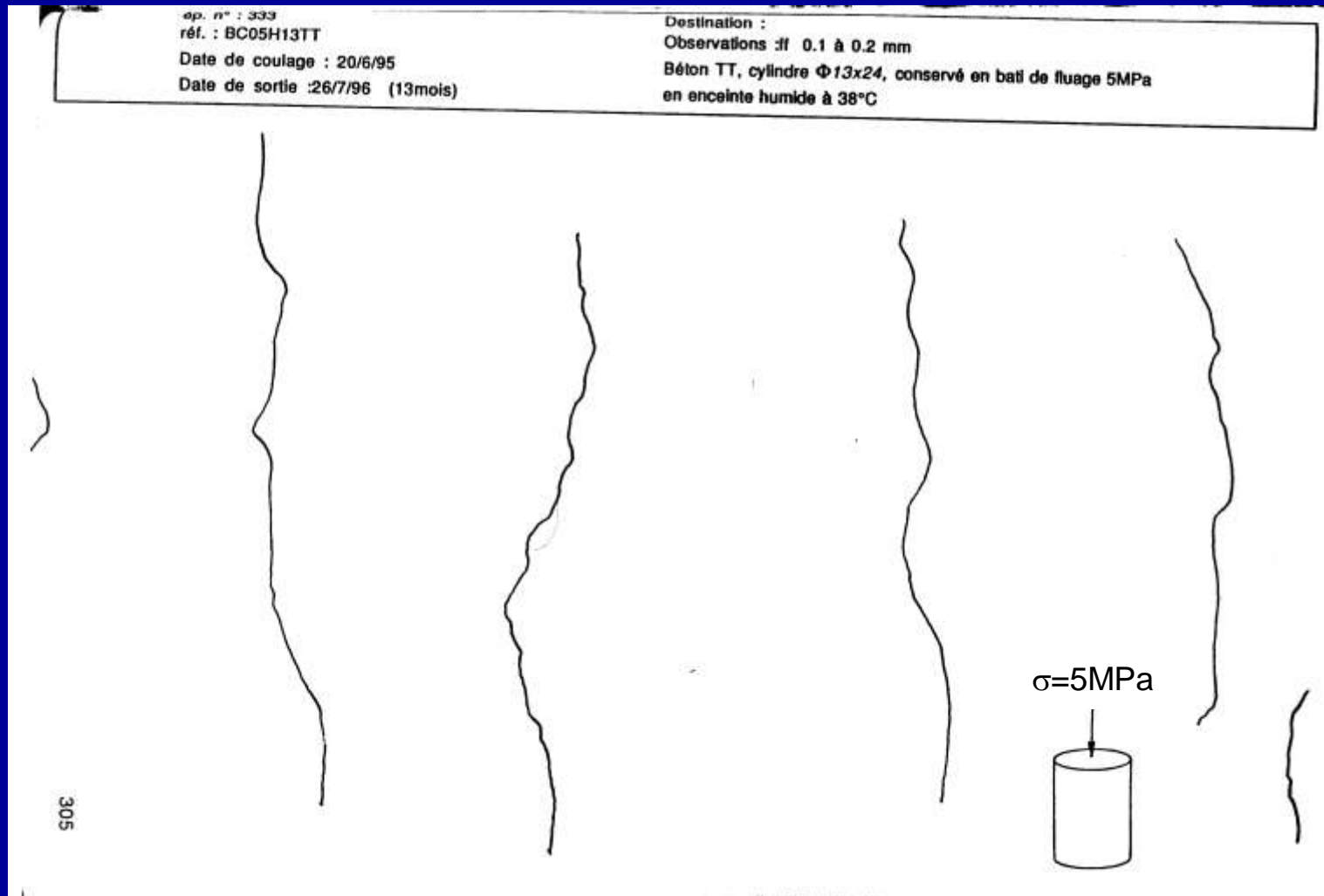
Cracking – free expansion



Cracking – free expansion

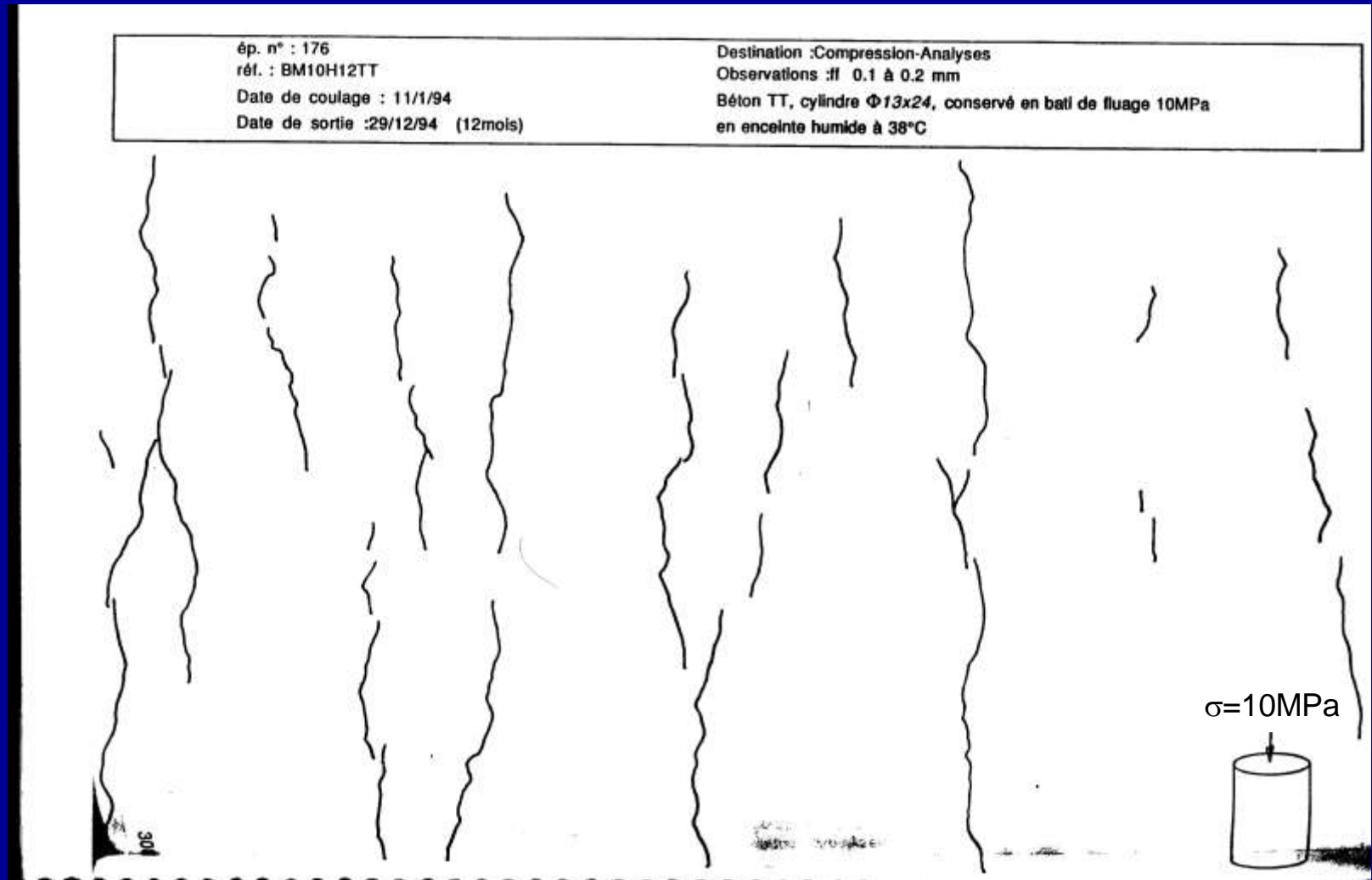


Stress induced anisotropy - Cracking – $\sigma = 5 \text{ MPa}$ - LCPC tests



(Larive, C., Apports combinés de l'alkali-réaction et de ses effets mécaniques, thèse de doctorat, E.N.P.C., Paris, France, 1997.)

Stress induced anisotropy - Cracking – $\sigma = 10$ MPa - LCPC tests



(Larive, C., Apports combinés de l'alkali-réaction et de ses effets mécaniques, thèse de doctorat, E.N.P.C., Paris, France, 1997.)

Stress induced
anisotropy



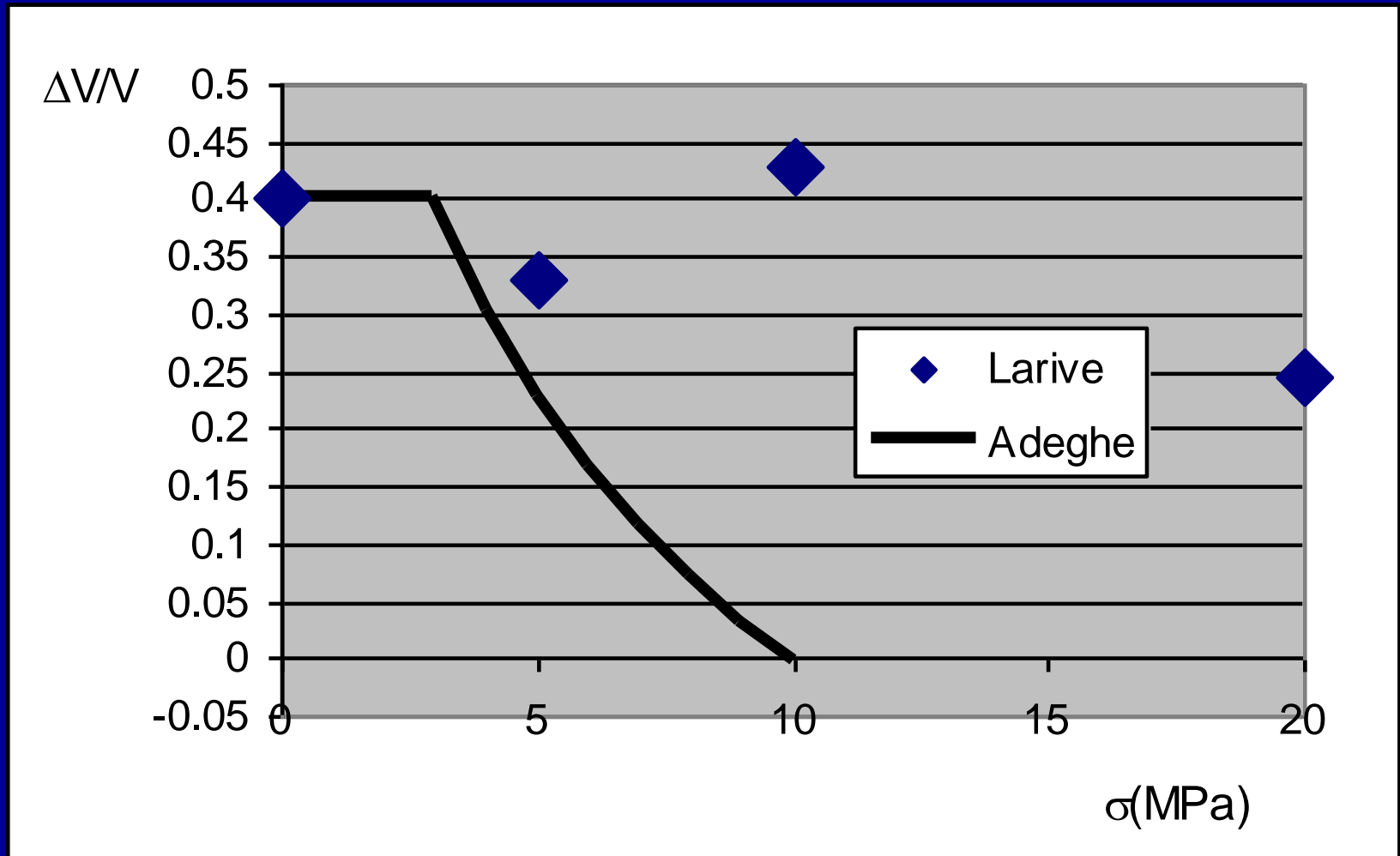
Stress induced anisotropy



Stress induced anisotropy

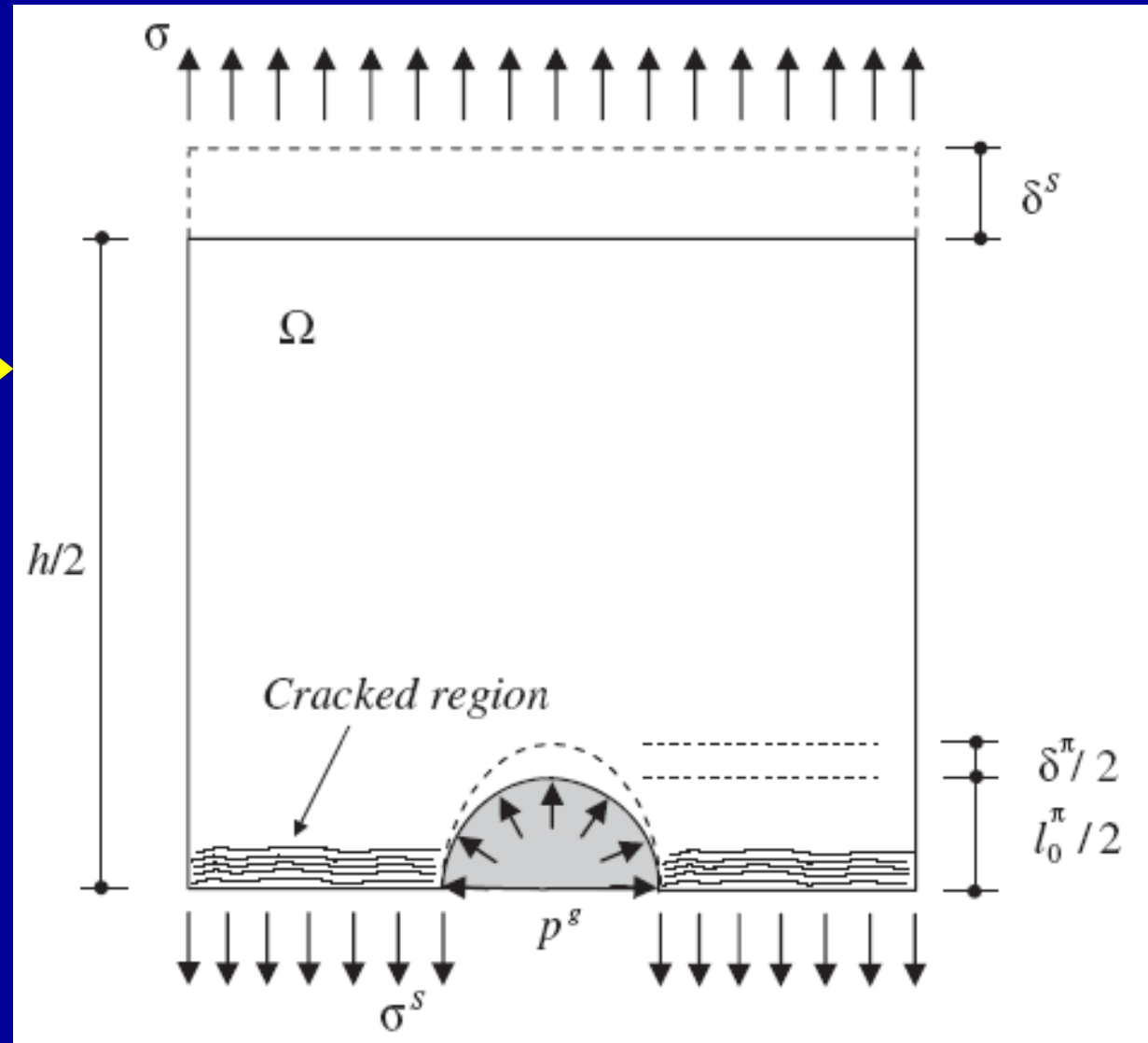
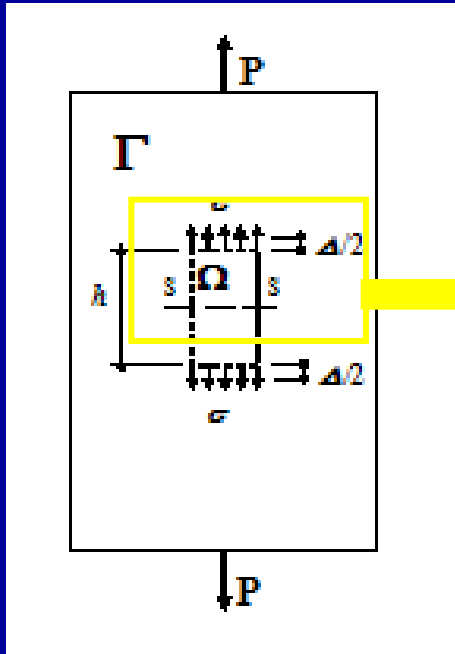


LCPC tests – for stresses levels until $\sigma = 10$ MPa $\Delta V/V$ does not change.



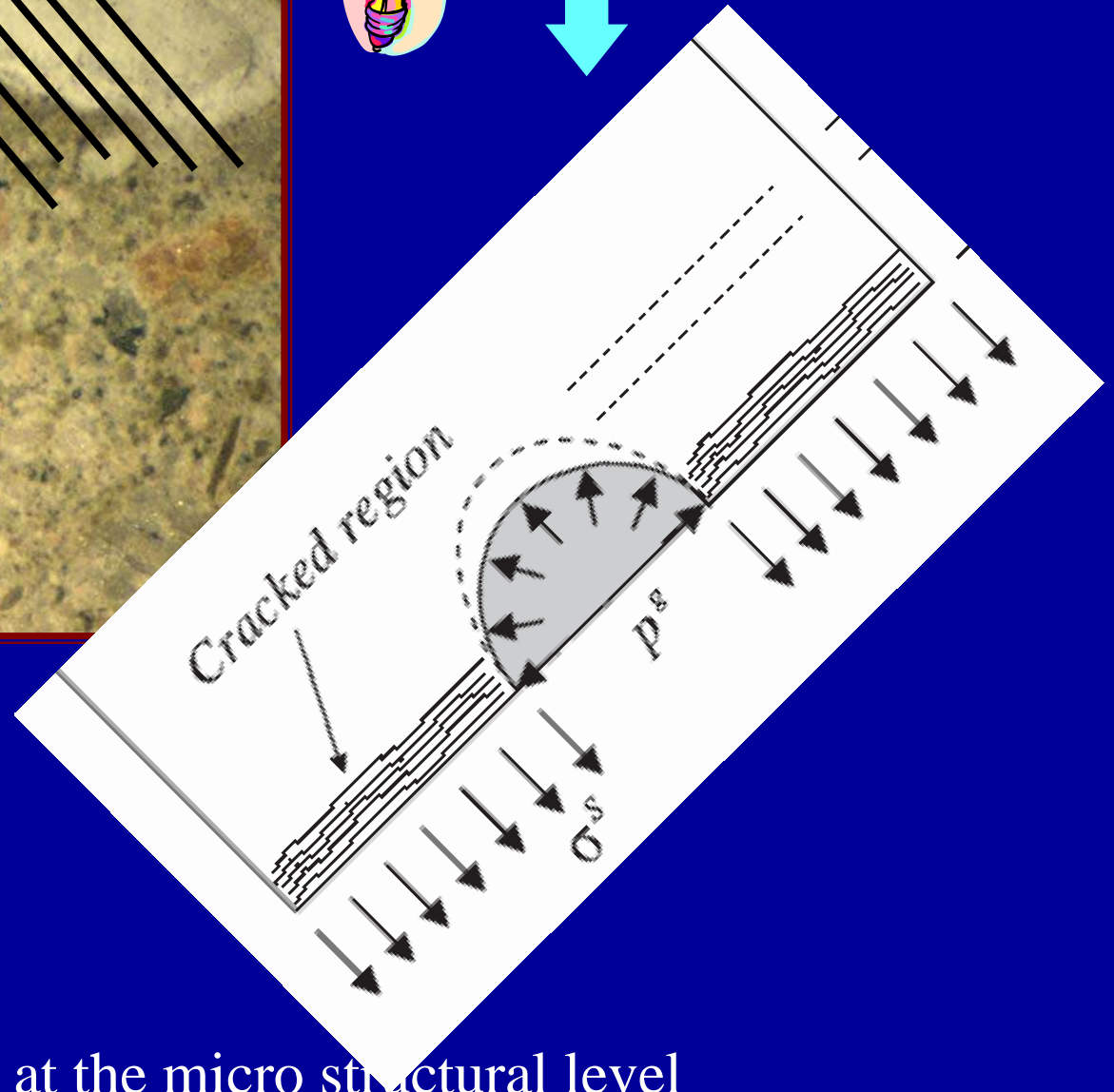
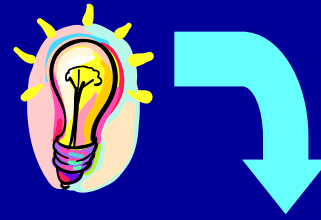
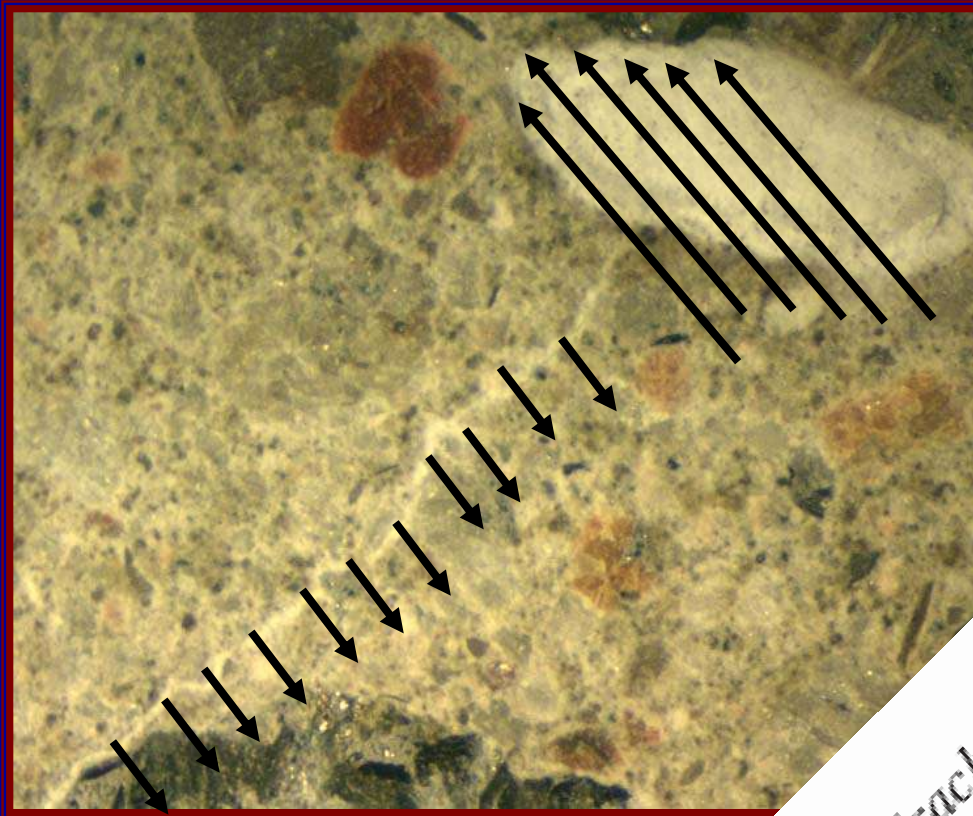
(Larive, C., Apports combinés de l'alkali-réaction et de ses effets mécaniques, thèse de doctorat, E.N.P.C., Paris, France, 1997.)

Mechanical model (1D think model)



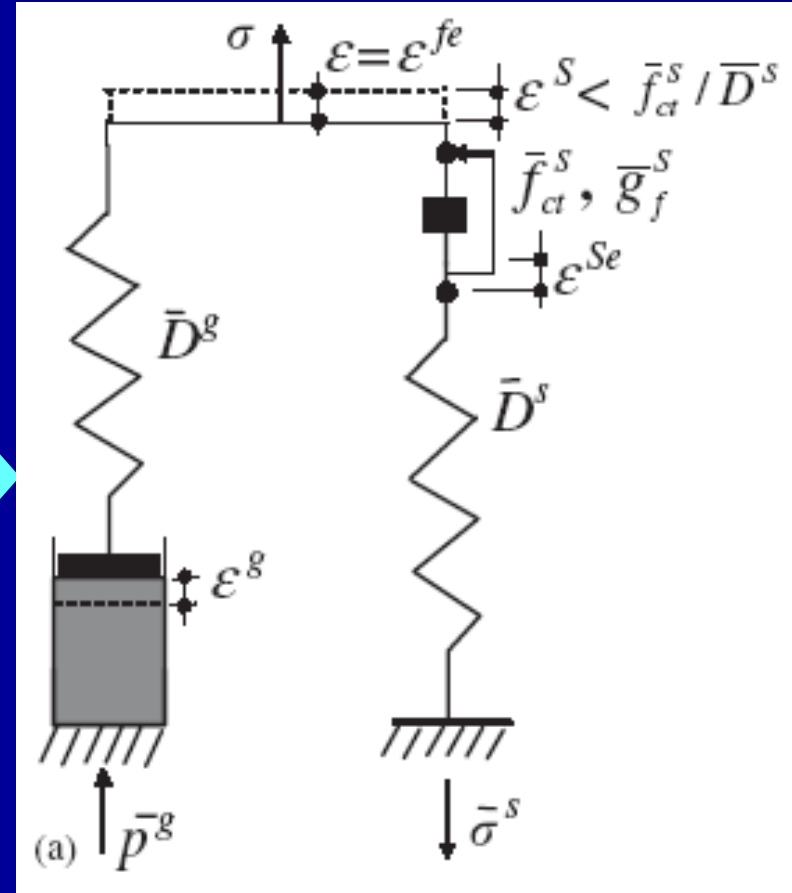
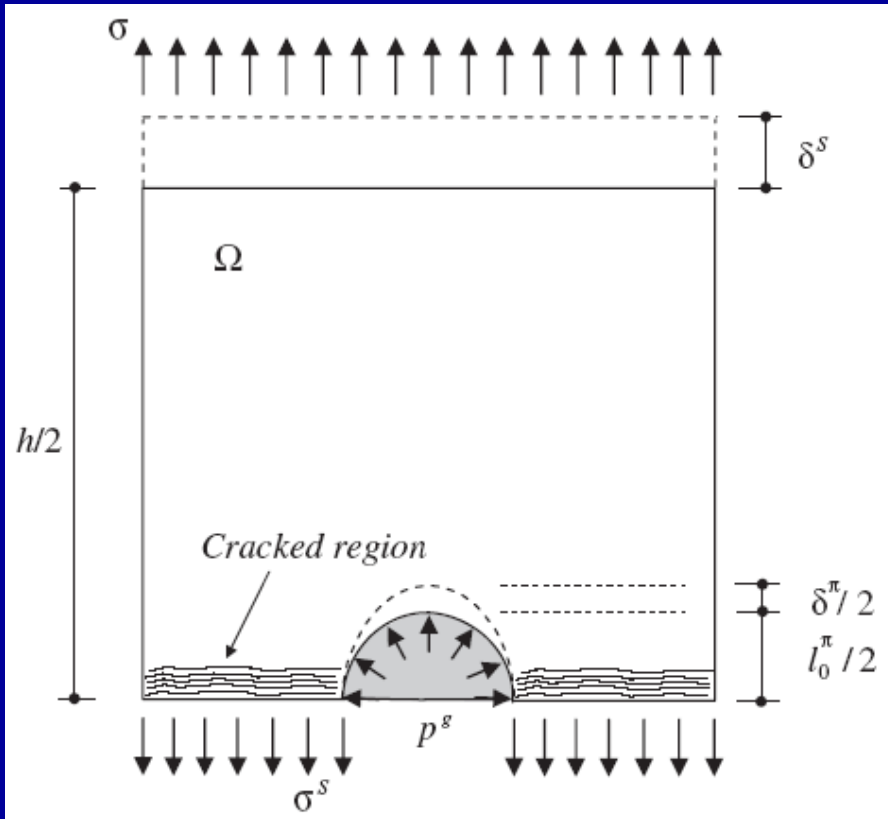
Model at the micro structural level

Mechanical model (1D think model)



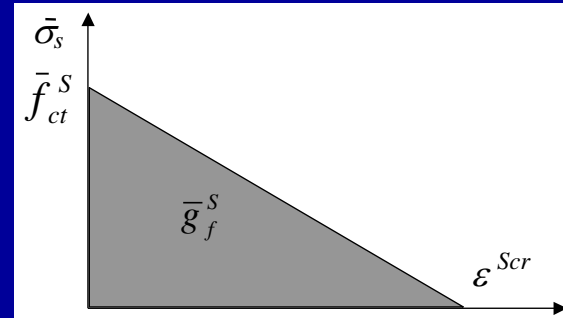
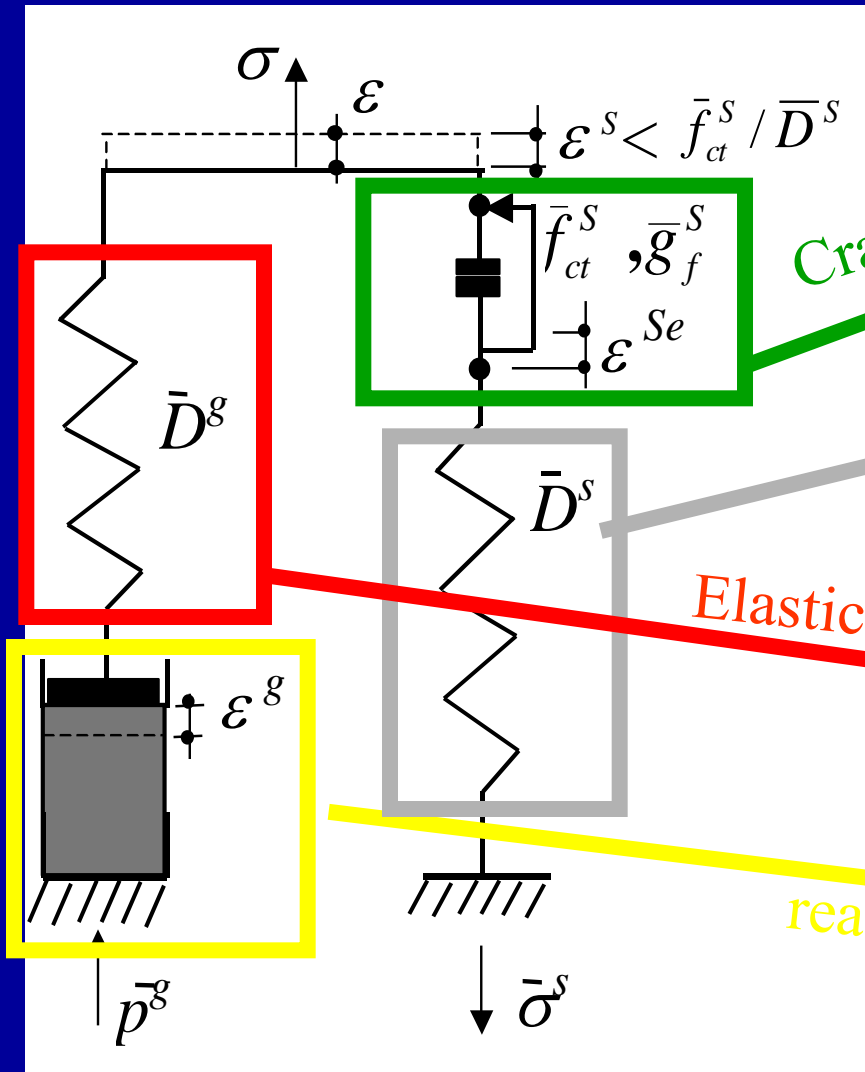
Model at the micro structural level

Thermo-chemo-mechanical model (1D think model)



The model is based on Ulm and Coussy (elastic and plastic) models

Thermo-chemo-mechanical model - cracking (1D think model)

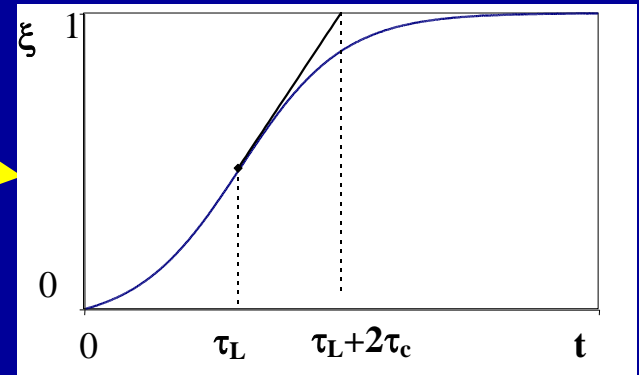
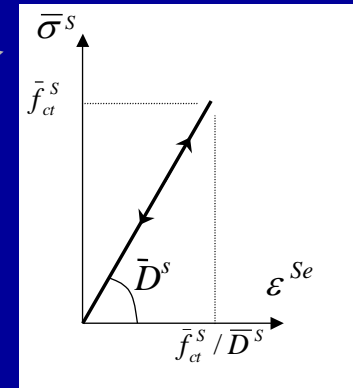
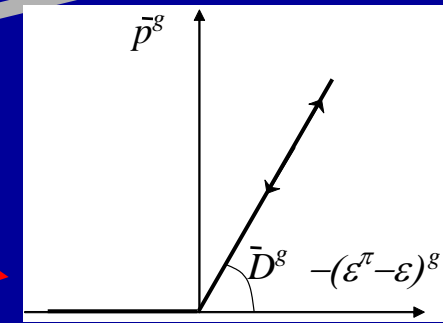


Cracking

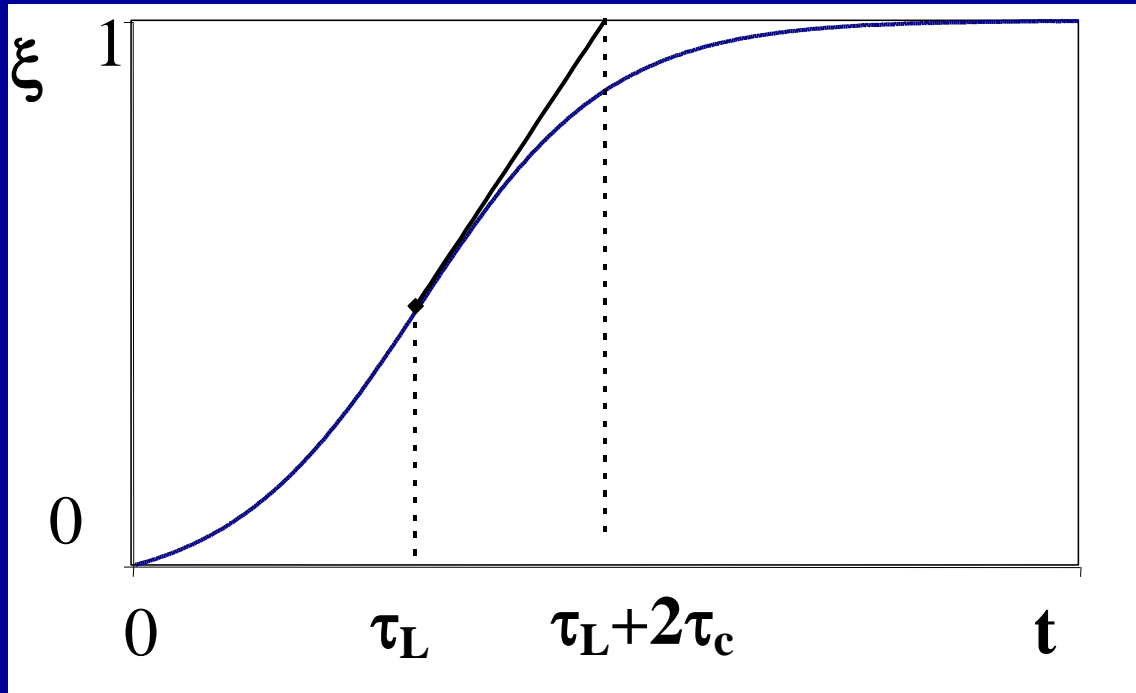
Elasticity

Elasticity

Chemical reaction: $\epsilon^g = k\xi$



Model (thermo-hygro-chemo-mechanical) for AAR
 The reaction depends on: umidity and temperature.



$$\xi(t) = \frac{1 - \exp(-t/\tau_c)}{1 + \exp(-t/\tau_c + \tau_L/\tau_c)}$$

$$\tau_c(\theta) = \tau_c(\theta_0) \exp[U_c(1/\theta - 1/\theta_0)]$$

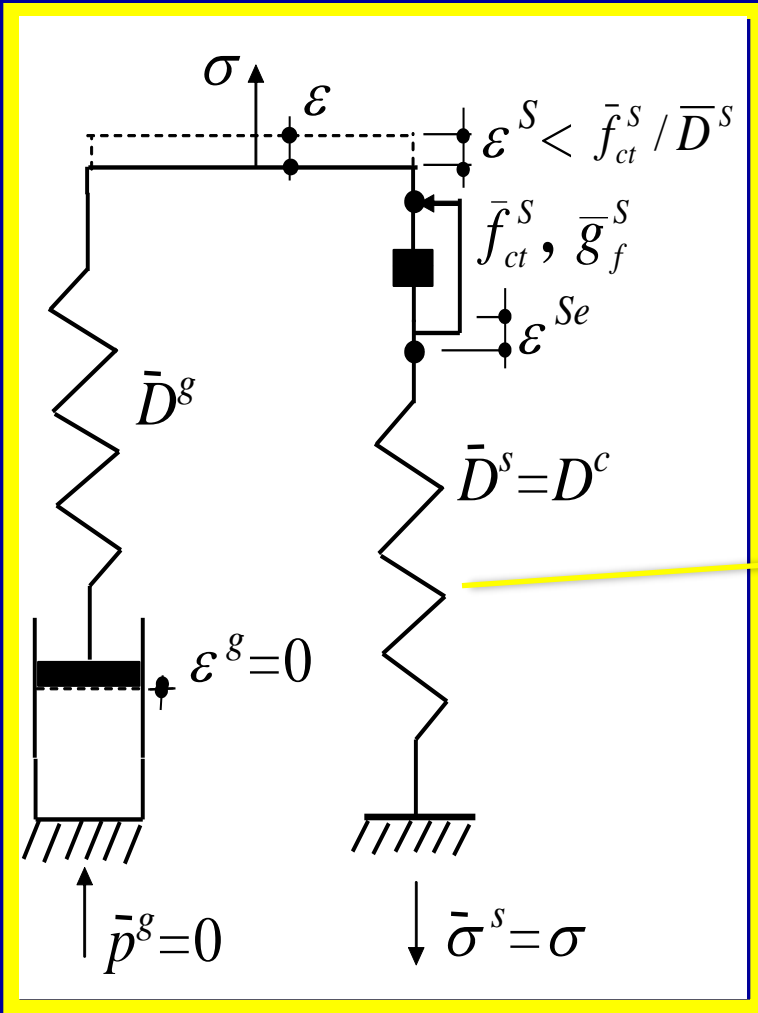
$$\tau_l(\theta) = \tau_l(\theta_0) \exp[U_l(1/\theta - 1/\theta_0)]$$

$$\varepsilon^g = k\xi$$

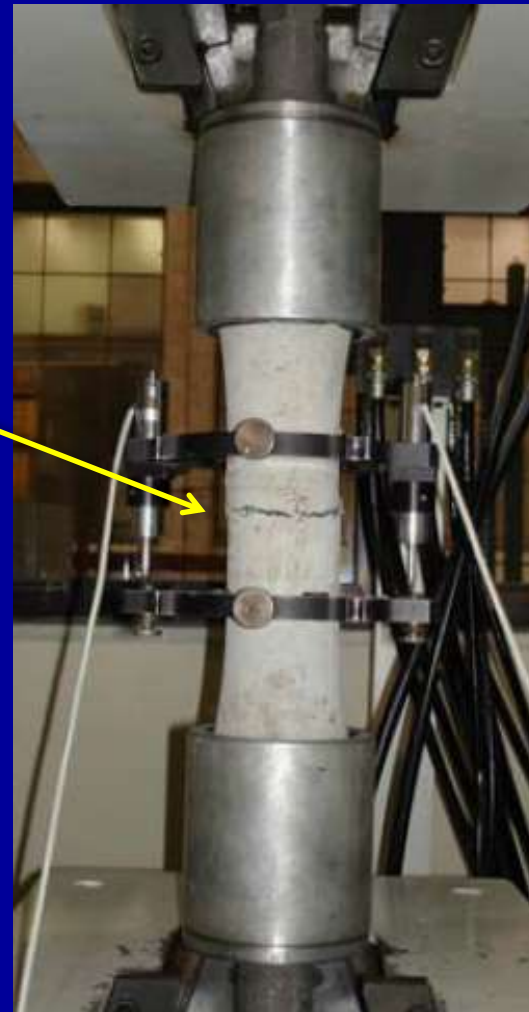
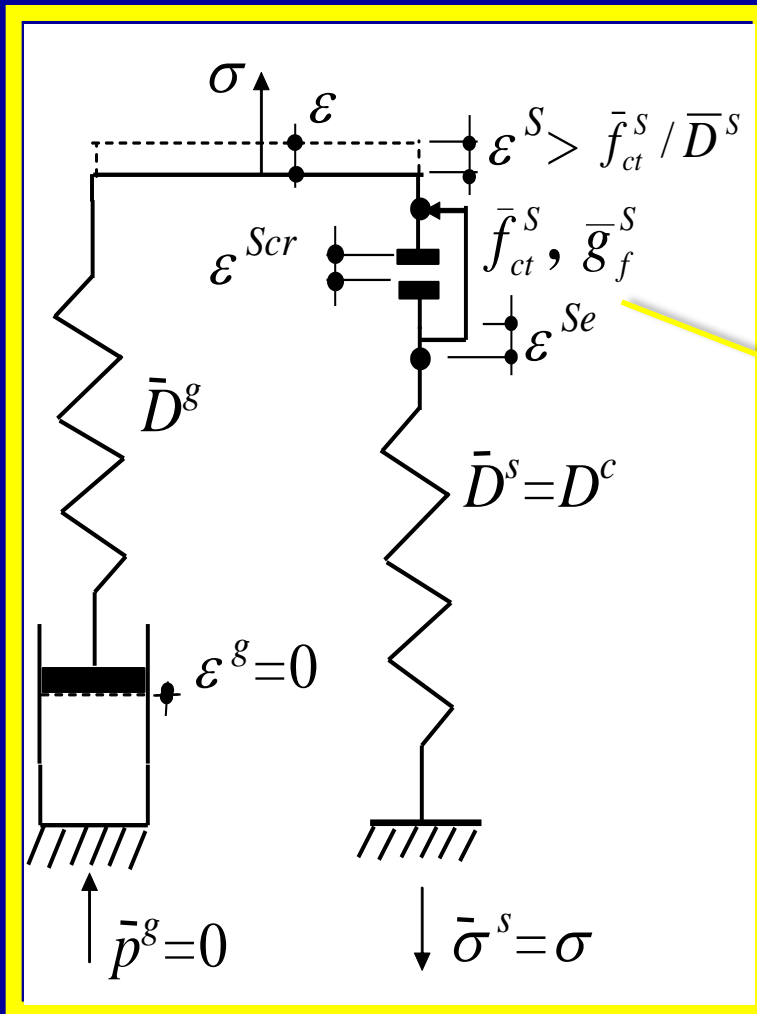
$$k = f(h)$$

Determination of parameters

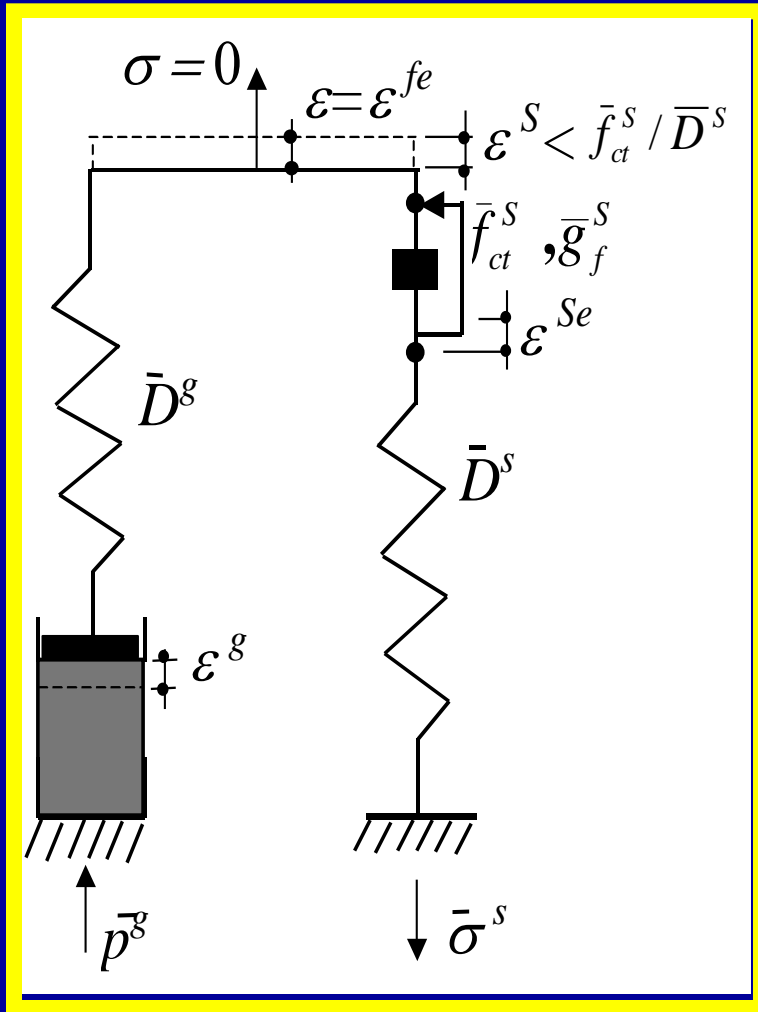
Test for the determination of Young's modulus



Test for the determination of fracture parameters

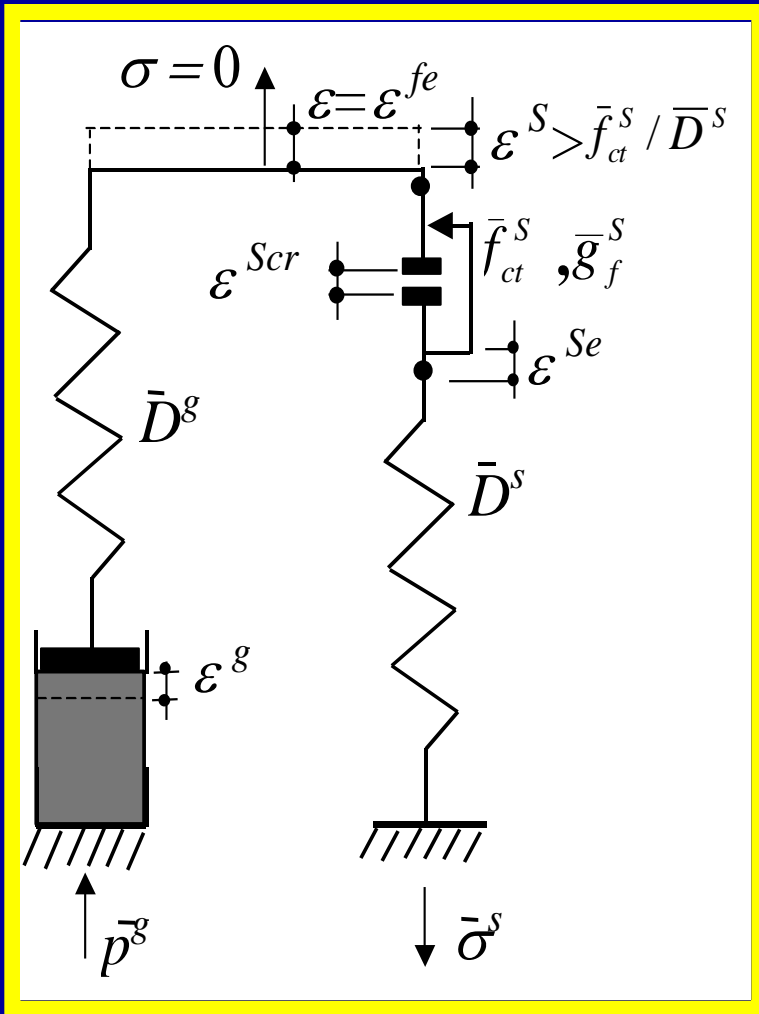


Test for the determination of AAR parameters – free expansion



Uncracked specmen

Test for the determination of AAR parameters – free expansion



Cracked specimen

Test for the determination of AAR parameters – free expansion



Robots (RMDV1 e RMDV2) for measuring volumetric delayed strains

Test for the determination of AAR parameters – free expansion



Laboratory dedicated to delayed strain measurements

Generalization: Classical fixed orthogonal smeared crack model

- Decomposition of total deformation for the cracked material in a crack deformation and in a deformation of the uncracked material between the cracks:

$$\dot{\boldsymbol{\varepsilon}} = \dot{\boldsymbol{\varepsilon}}^S = \dot{\boldsymbol{\varepsilon}}^{Se} + \dot{\boldsymbol{\varepsilon}}^{Scr}$$

Stresses equilibrium:

$$\dot{\boldsymbol{\sigma}} = \dot{\boldsymbol{\sigma}}^S - \dot{p}_g \mathbf{1}$$

Constitutive relations for the gel and for the skeleton:

$$\dot{p}^g = \bar{K}^g \langle -(\dot{\boldsymbol{\varepsilon}}^V - \dot{\boldsymbol{\varepsilon}}^{g,V}) \rangle$$

$$\dot{\boldsymbol{\sigma}}^S = \bar{\mathbf{D}}^S \dot{\boldsymbol{\varepsilon}}^{Se}$$

Overall stress-strain relation:

$$\dot{\boldsymbol{\sigma}}^S = \bar{\mathbf{D}}^{S,Scr} \dot{\boldsymbol{\varepsilon}}^S$$

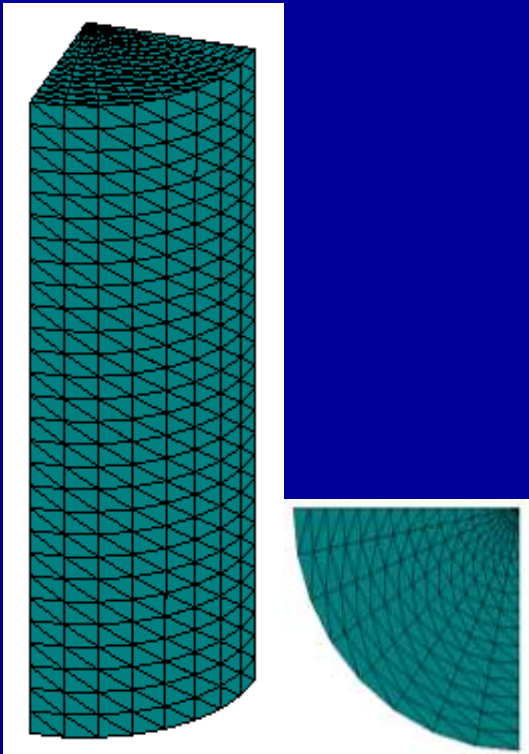
$$\bar{\mathbf{D}}^{S,Scr} = \left[\bar{\mathbf{D}}^S - \bar{\mathbf{D}}^S \mathbf{N} \left(\hat{\mathbf{D}}^{Scr} + \mathbf{N}^T \bar{\mathbf{D}}^S \mathbf{N} \right)^{-1} \mathbf{N}^T \bar{\mathbf{D}}^S \right]$$

Implementation: FEM 3D code

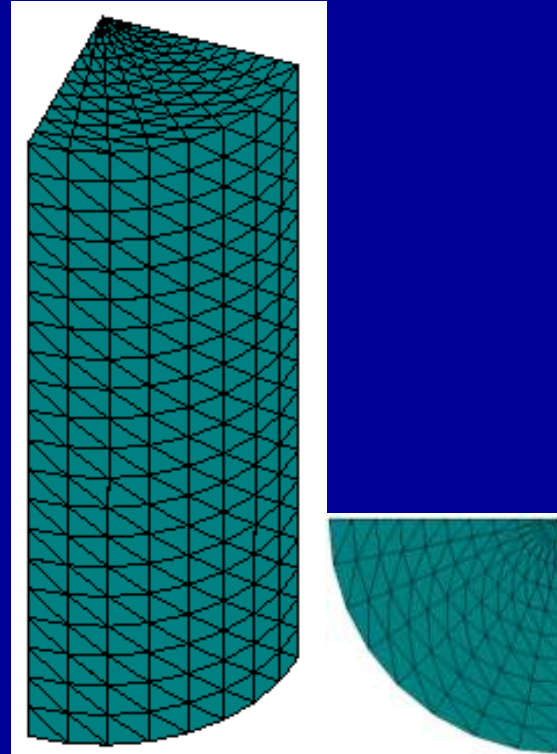
The model was implemented in a reference program developed in FORTRAN for non-linear analysis of three dimensional problems via Finite Element Method through four nodes tetrahedral elements. The resulting non-linear equations system is solved by means of a Newton-Raphson iterative-incremental technique. The initial stiffness matrix is used as an approximation for the discrete Jacobian. The solution of the linearized system employs the Pre-Conditioned Conjugated Gradients Method, which was implemented under an Element-By-Element technique avoiding global stiffness matrix assembling and factorization.

Validation: Larive's tests (LCPC – France)

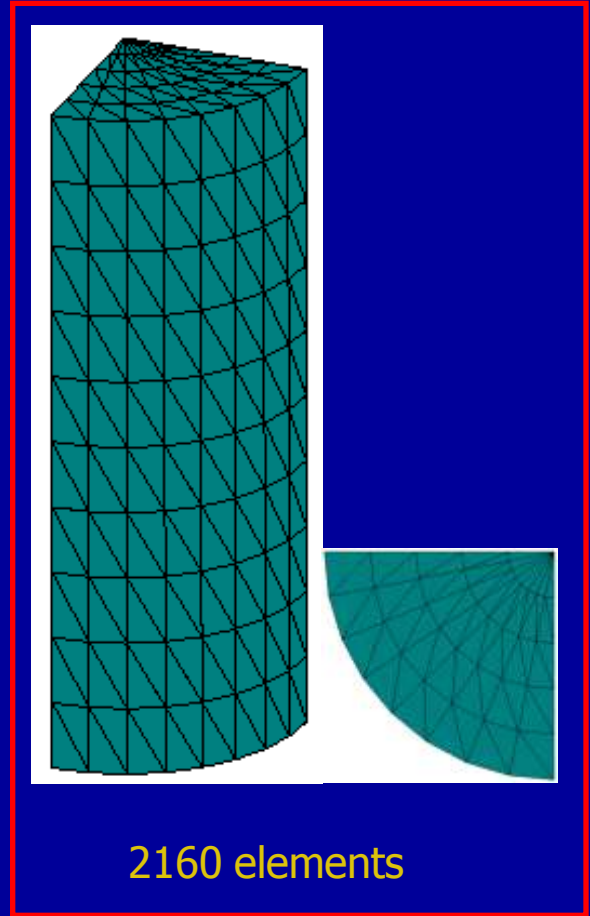
Validation: Larive's tests



18144 elements



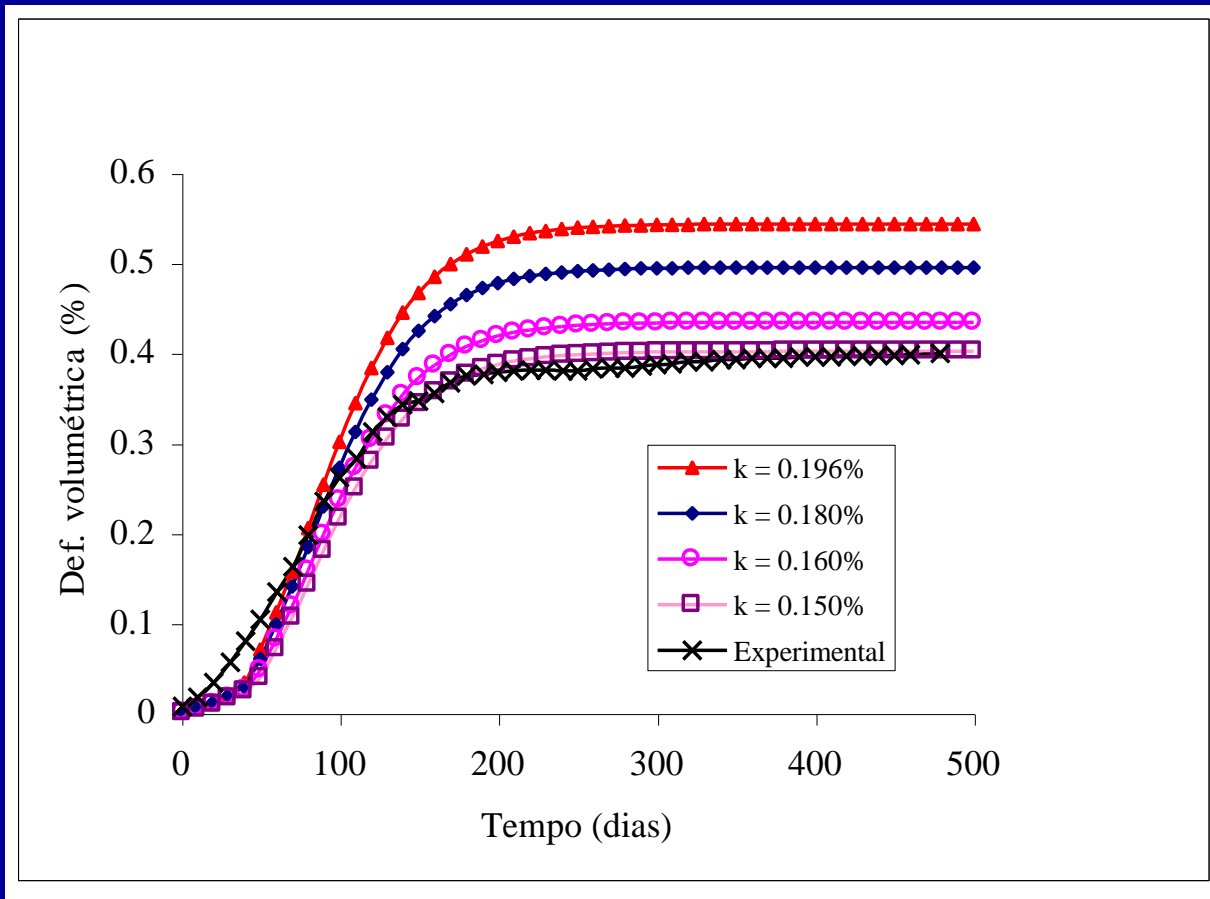
9120 elements



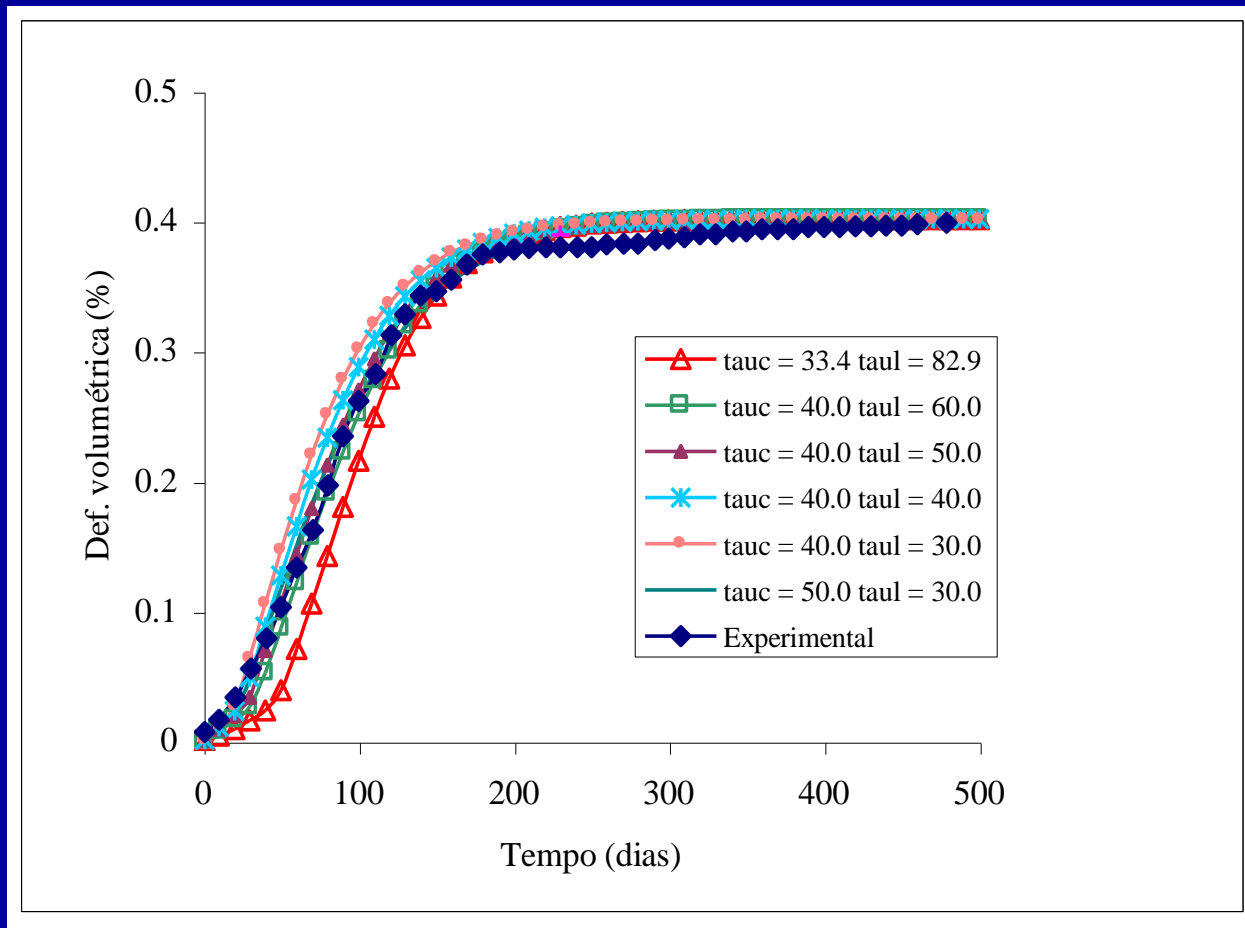
2160 elements

(FEM convergence test)

Inverse analysis: amplitude

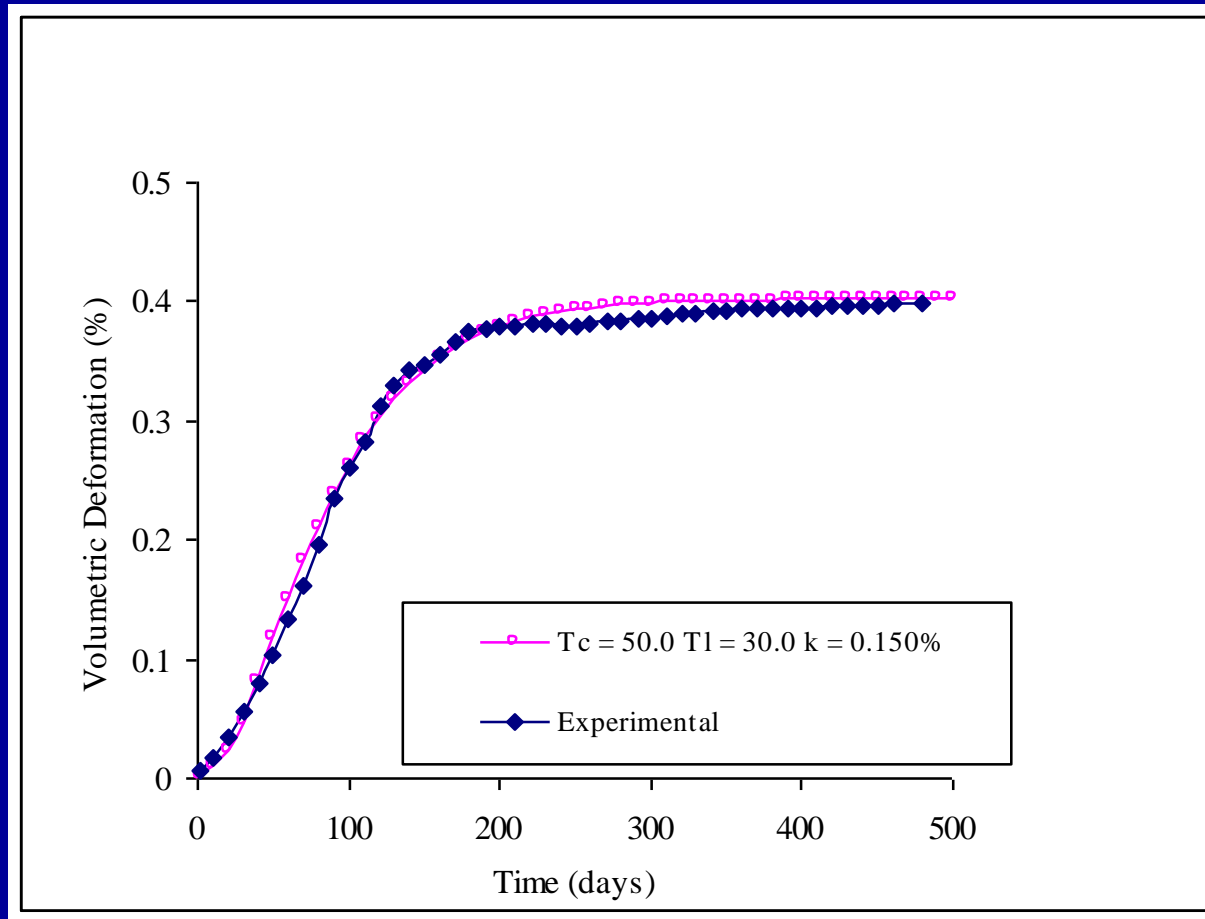


Inverse analysis: kinetics



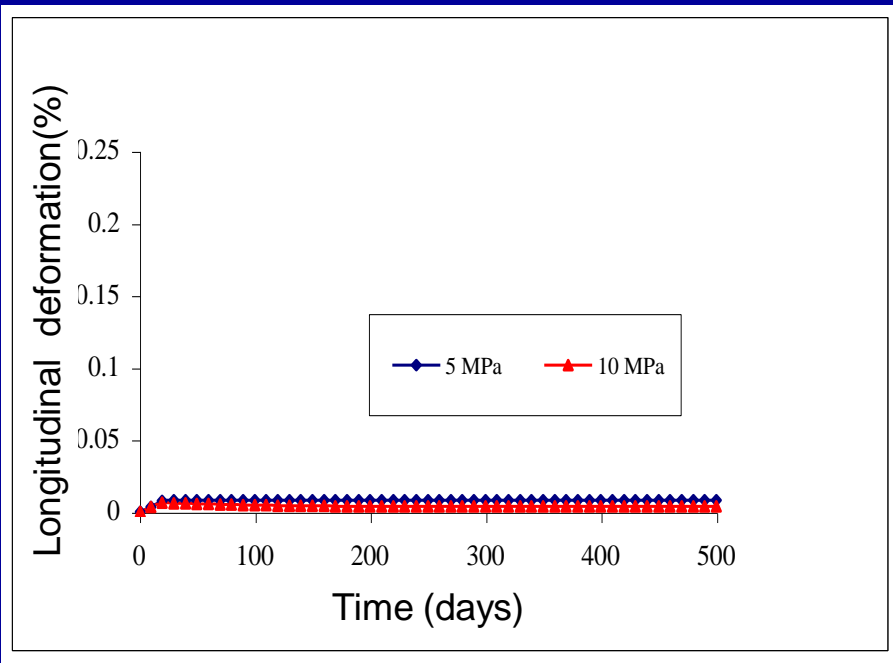
LCPC Larive's tests

Numerical and experimental results

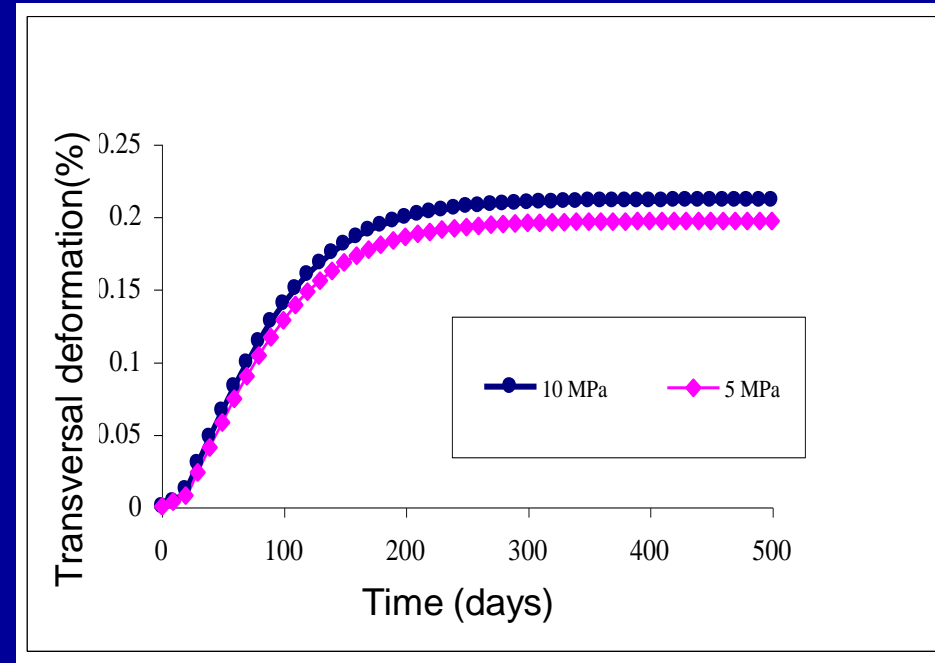


Numerical simulation of LCPC Larive's tests

Displaying stress-induced anisotropy



Longitudinal deformation



Transversal deformation

Simulation: hypothetical discharge ring

Simulation: hypothetical discharge ring

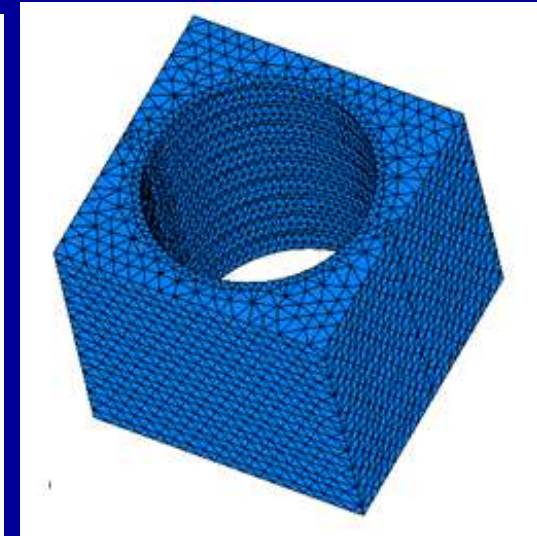
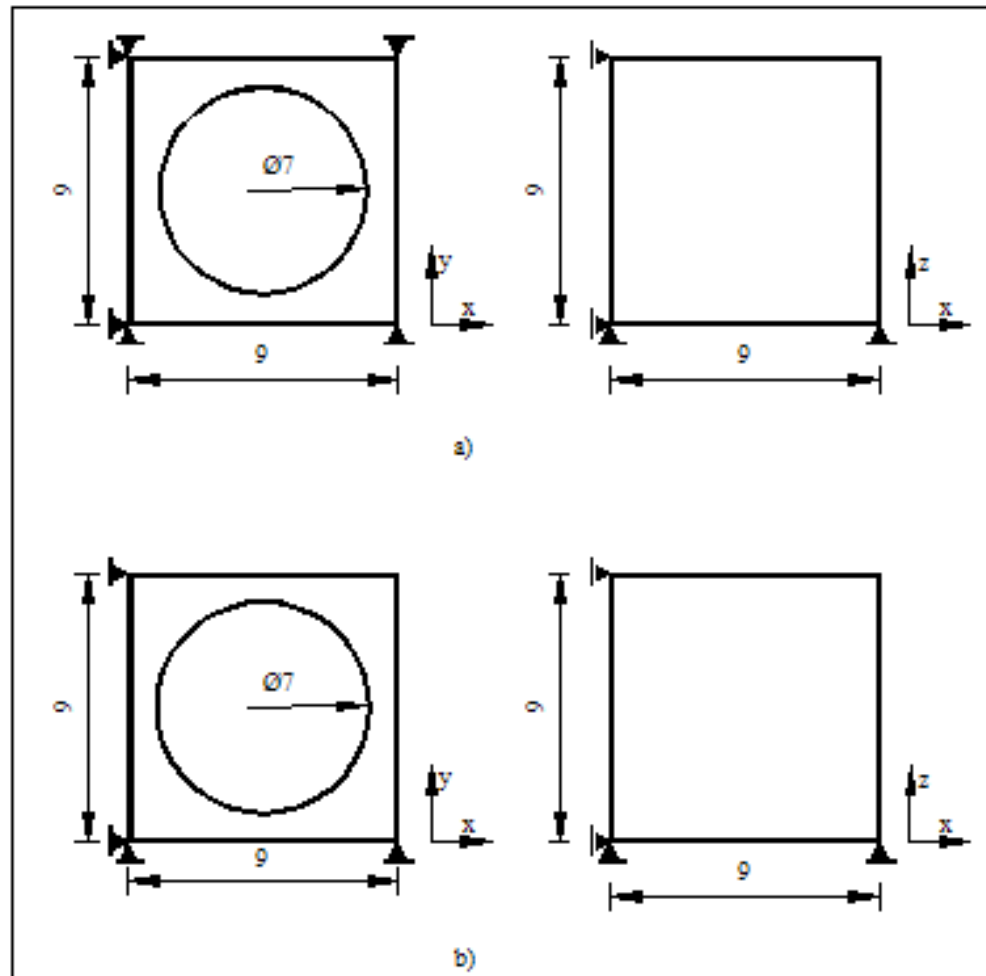


Figura 4.13- Geometria e condições de contorno: a) iniciais; b) após a abertura da junta

Simulation: hypothetical discharge ring

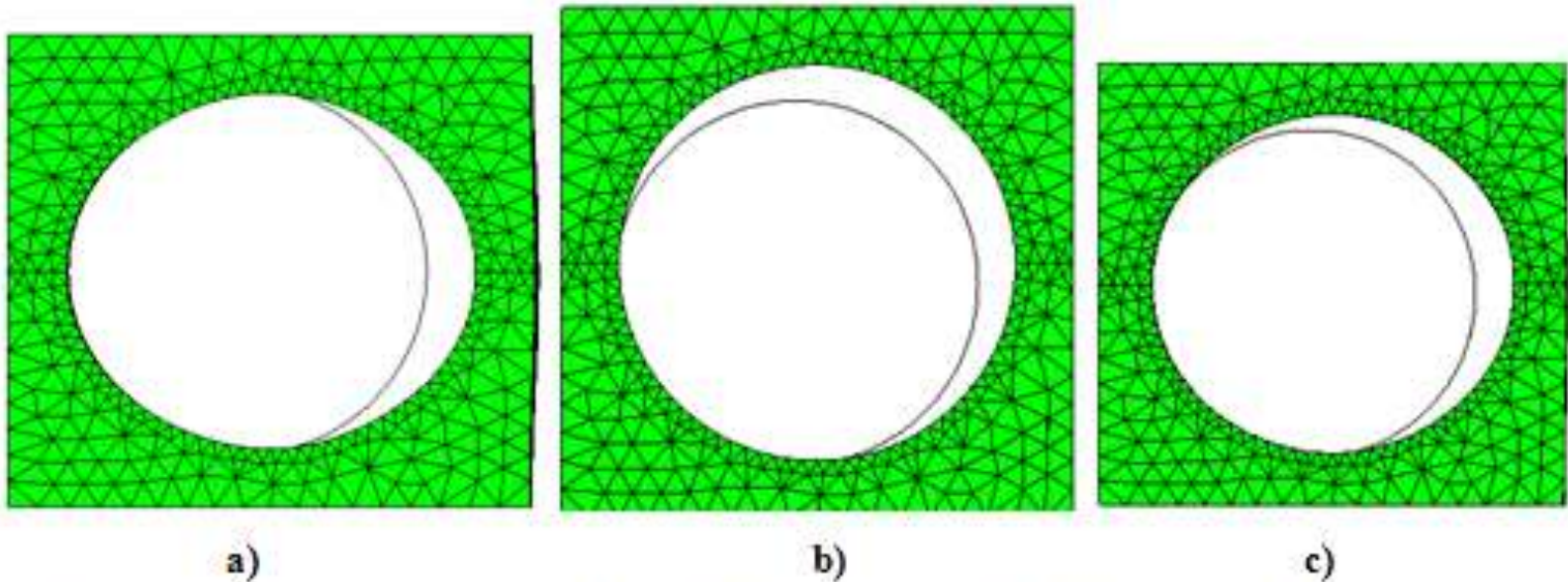


Figura 4.26– Configuração deformada: a) Sem junta de dilatação; b) Abertura da junta de dilatação aos 4 anos; c) Abertura da junta aos 10 anos.

Application: Furnas - 1.2 MW hydroelectric
power plant in
Minas Gerais - Brazil

Application – FURNAS dam





Application – FURNAS dam



(upstream view)

Application –FURNAS dam



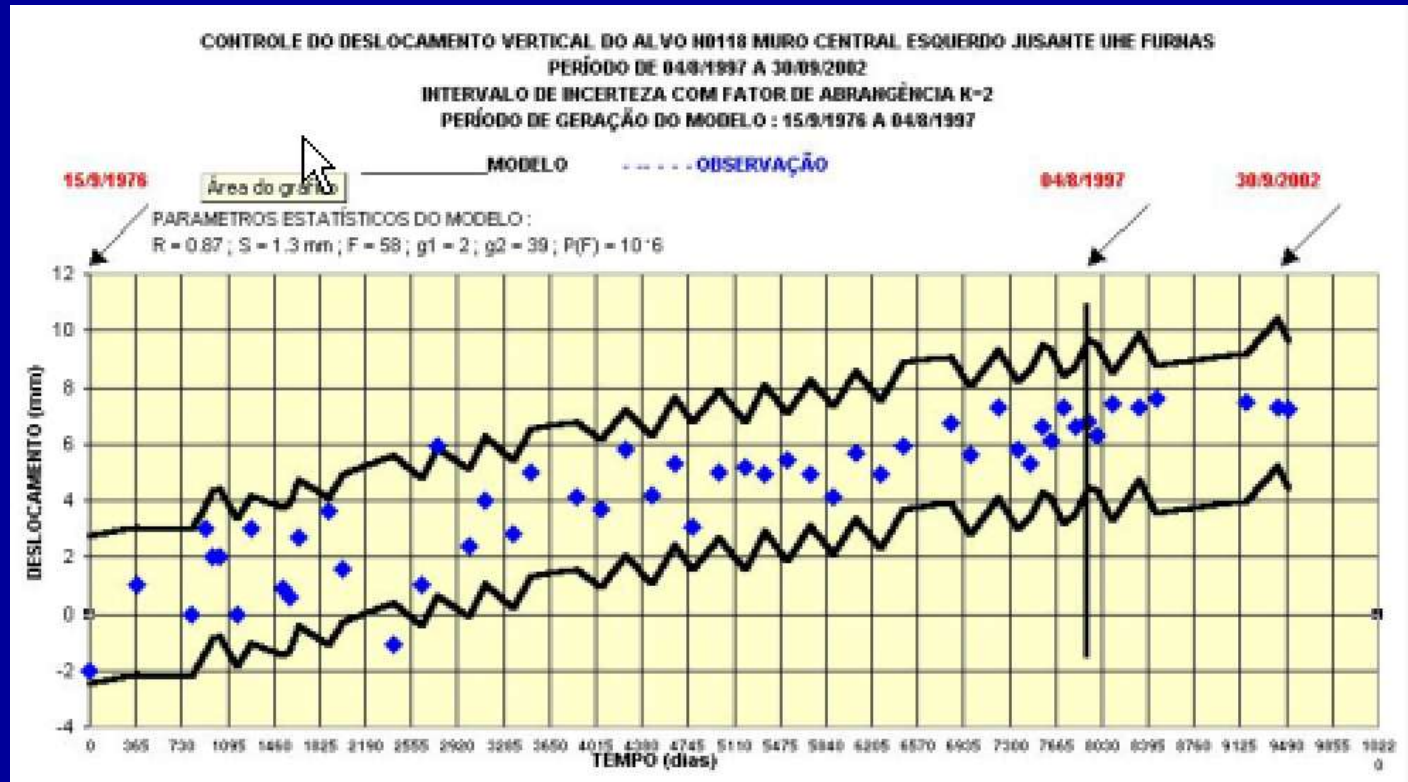
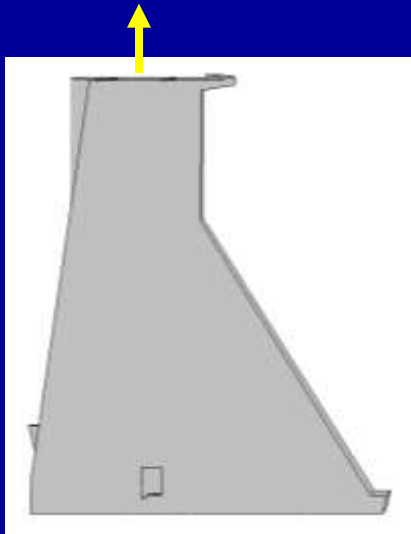
(downstream view)

Field measurements



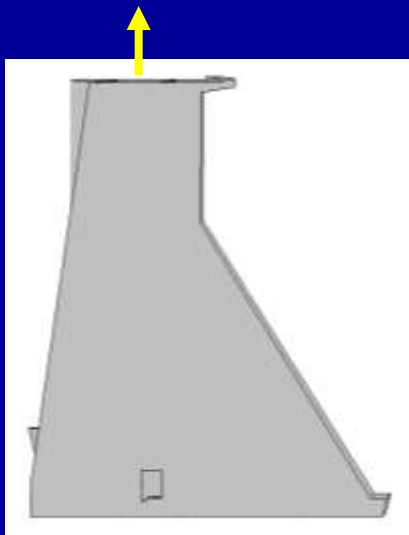
FURNAS dam

Field measurements: displacements at the crest



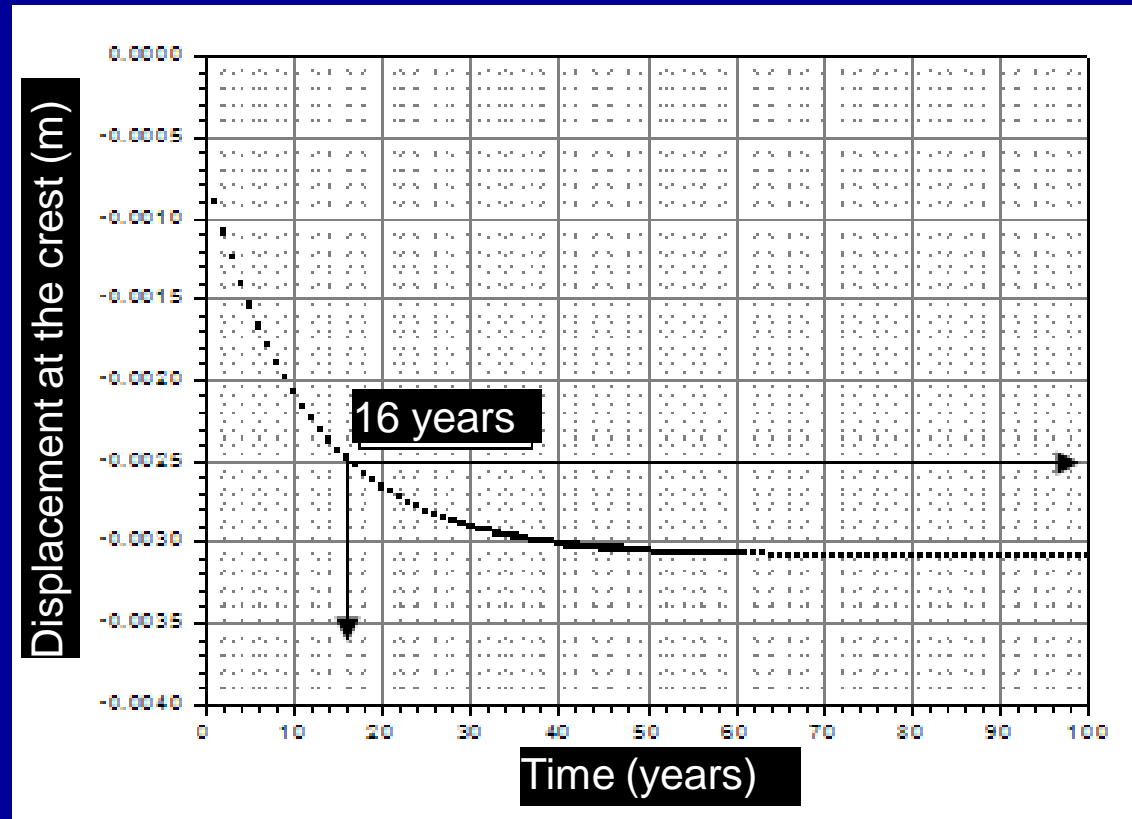
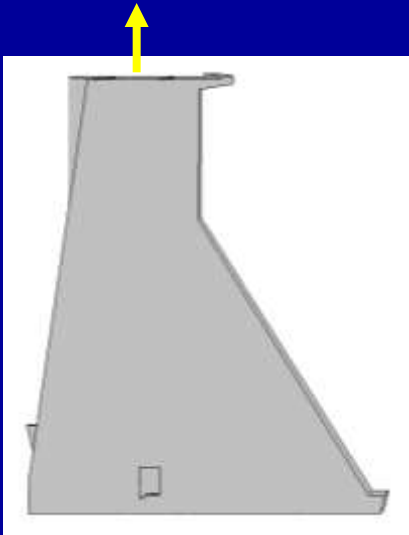
FURNAS dam

Field measurements: displacements at the crest: statistical modeling

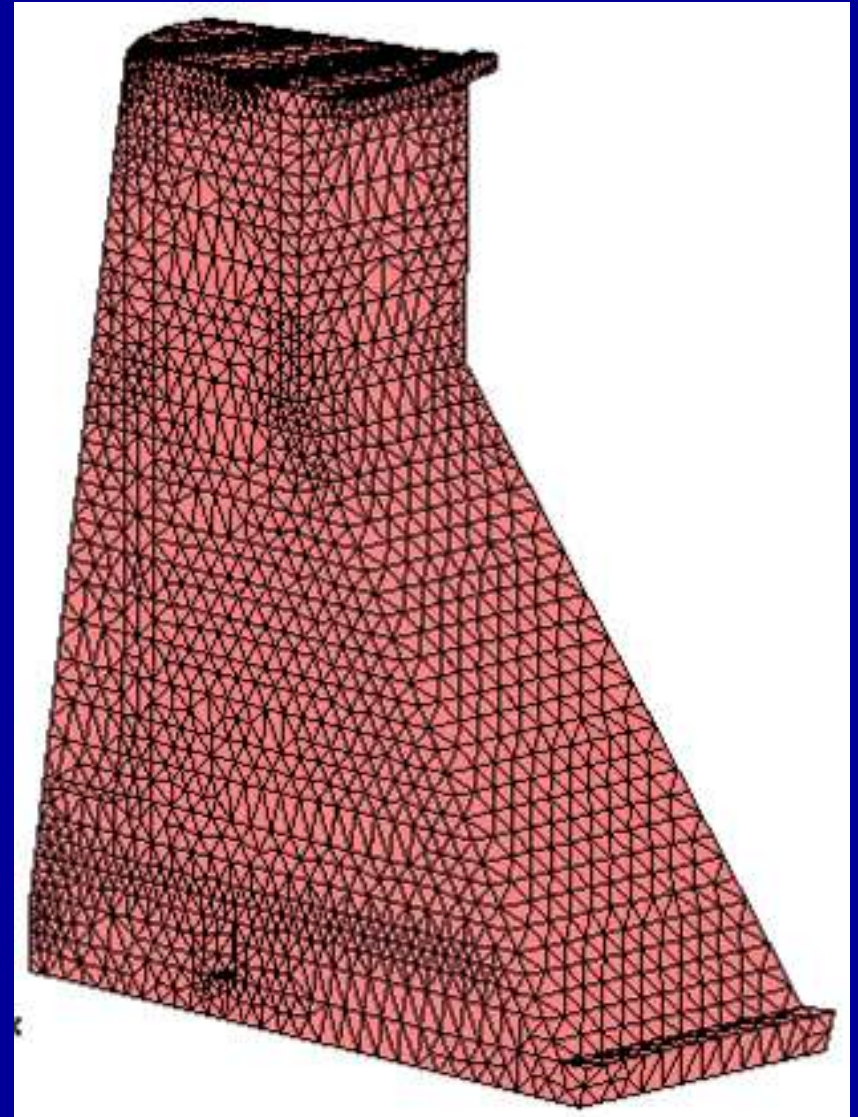
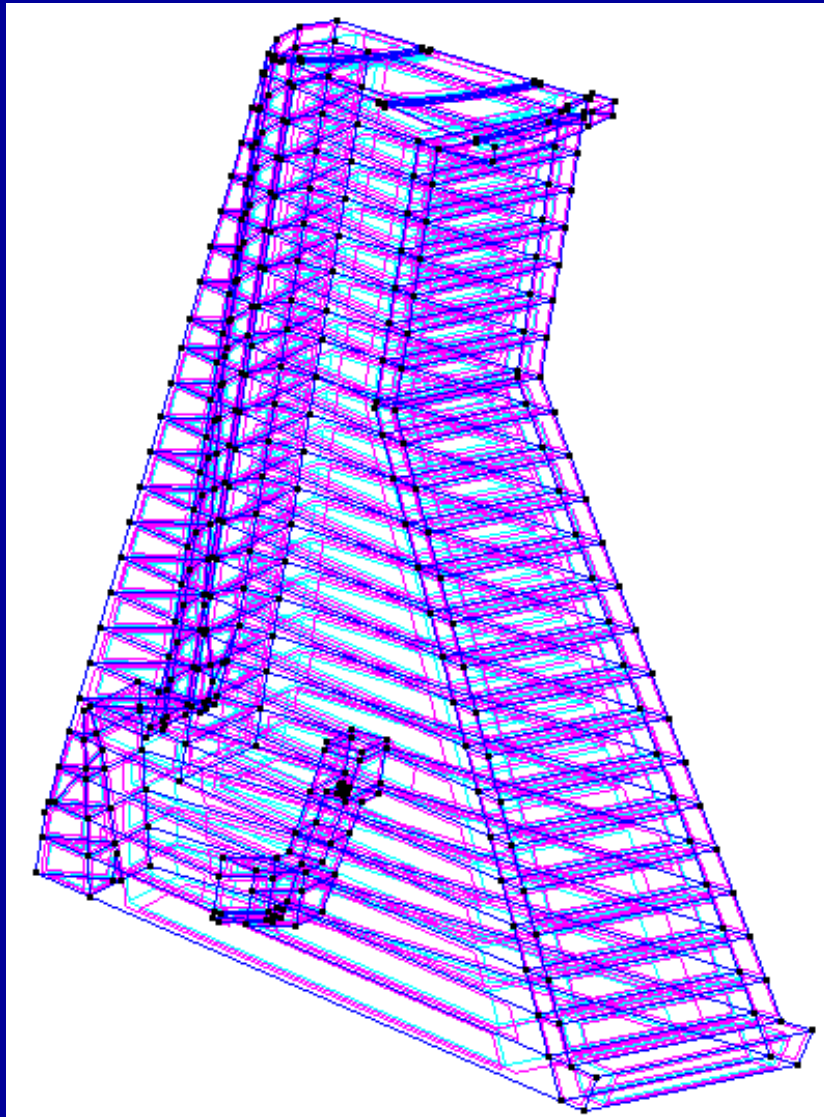


FURNAS dam

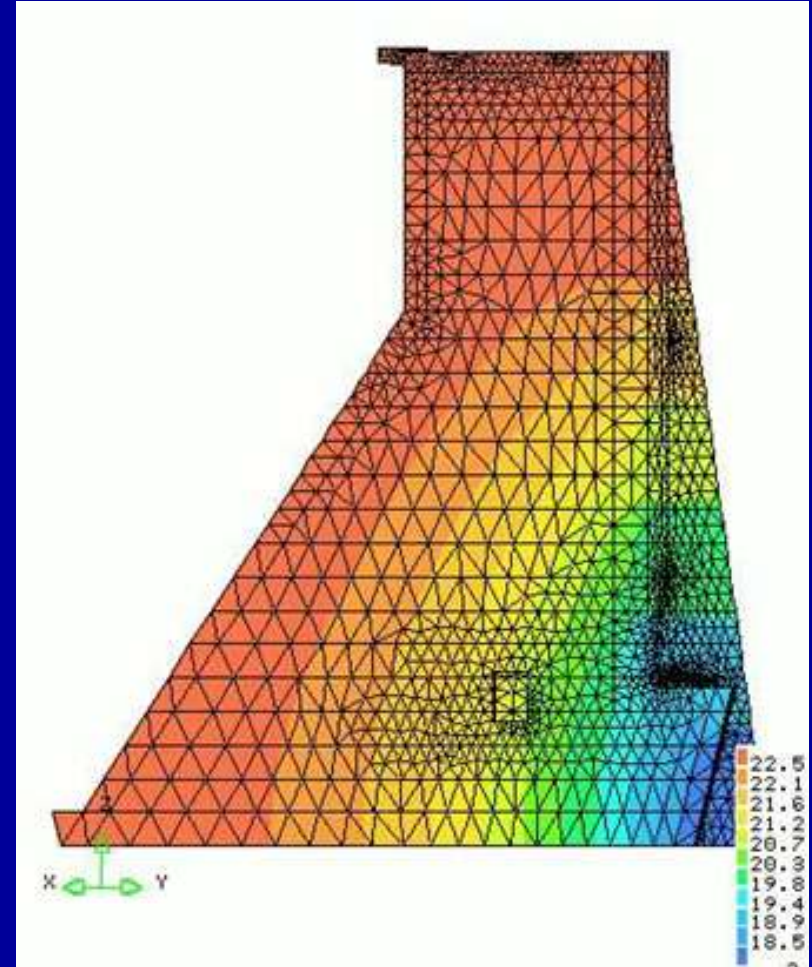
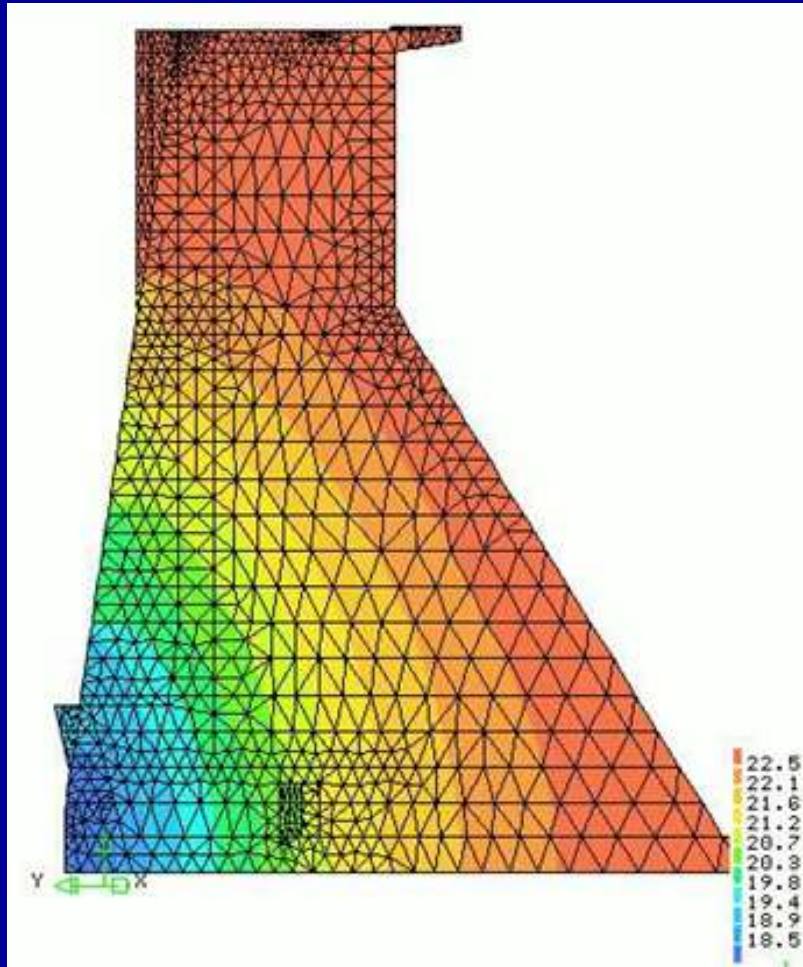
Displacements at the crest (m) : creep simulation



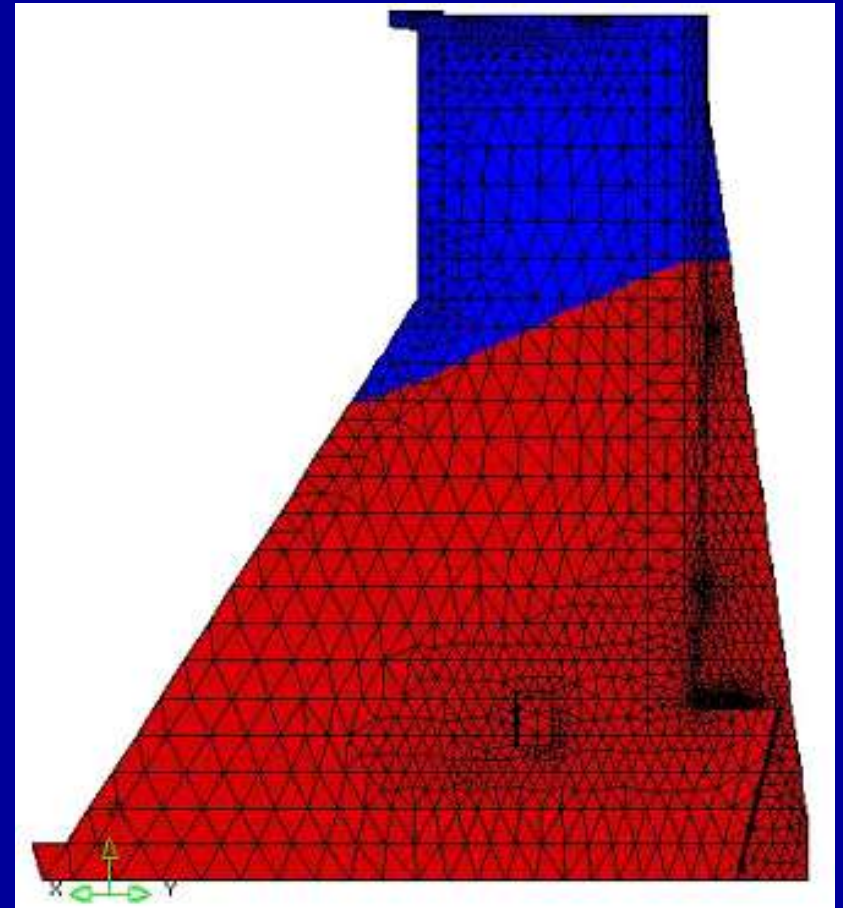
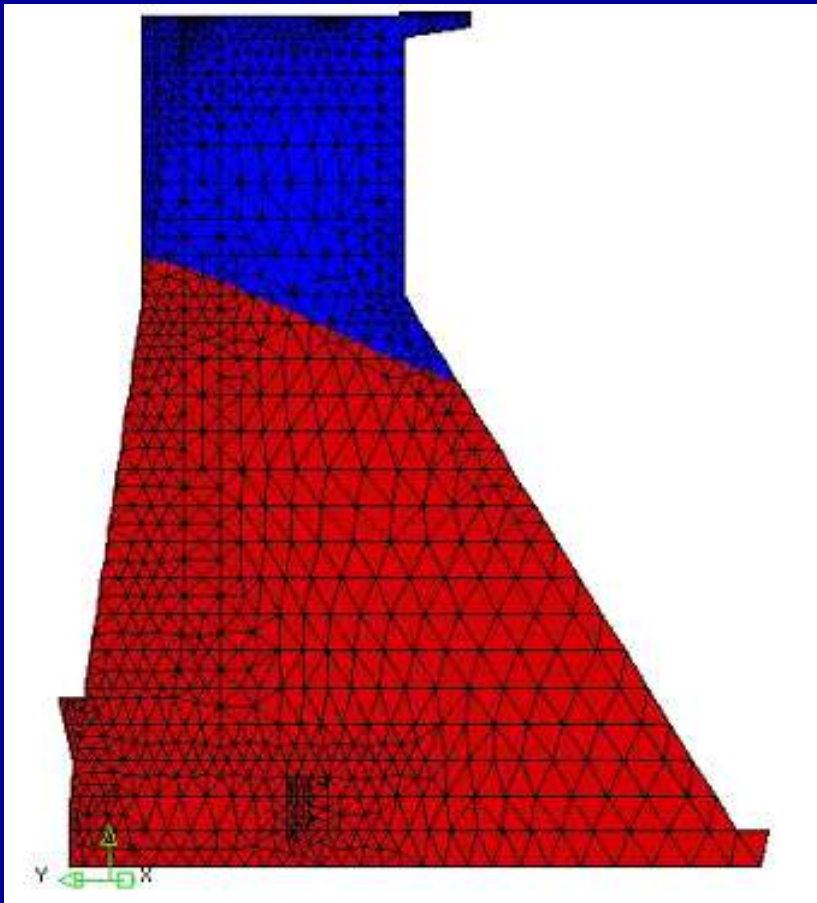
Furnas dam: FEM modeling – 49513 tetrahedral elements



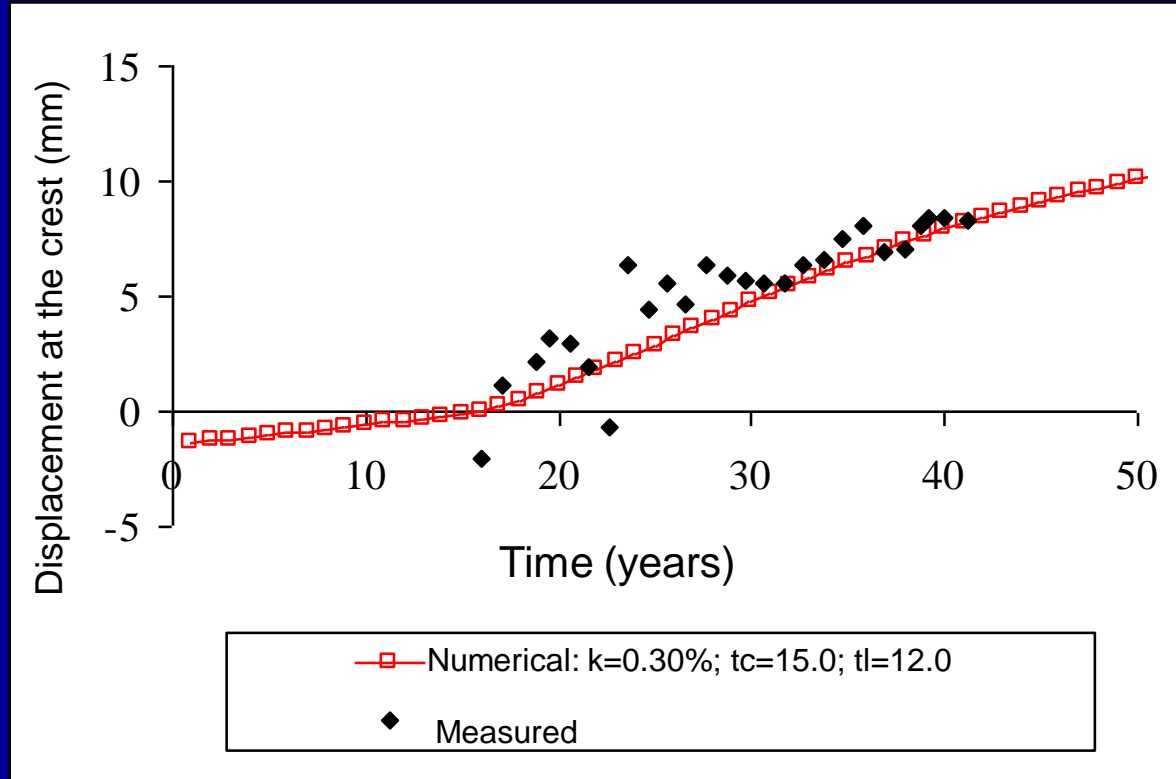
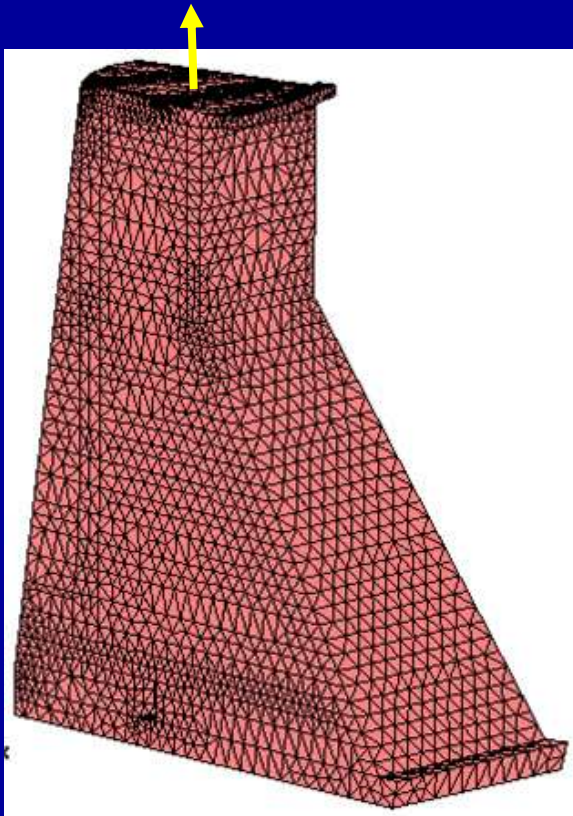
Furnas dam: thermal fields – averaged steady state



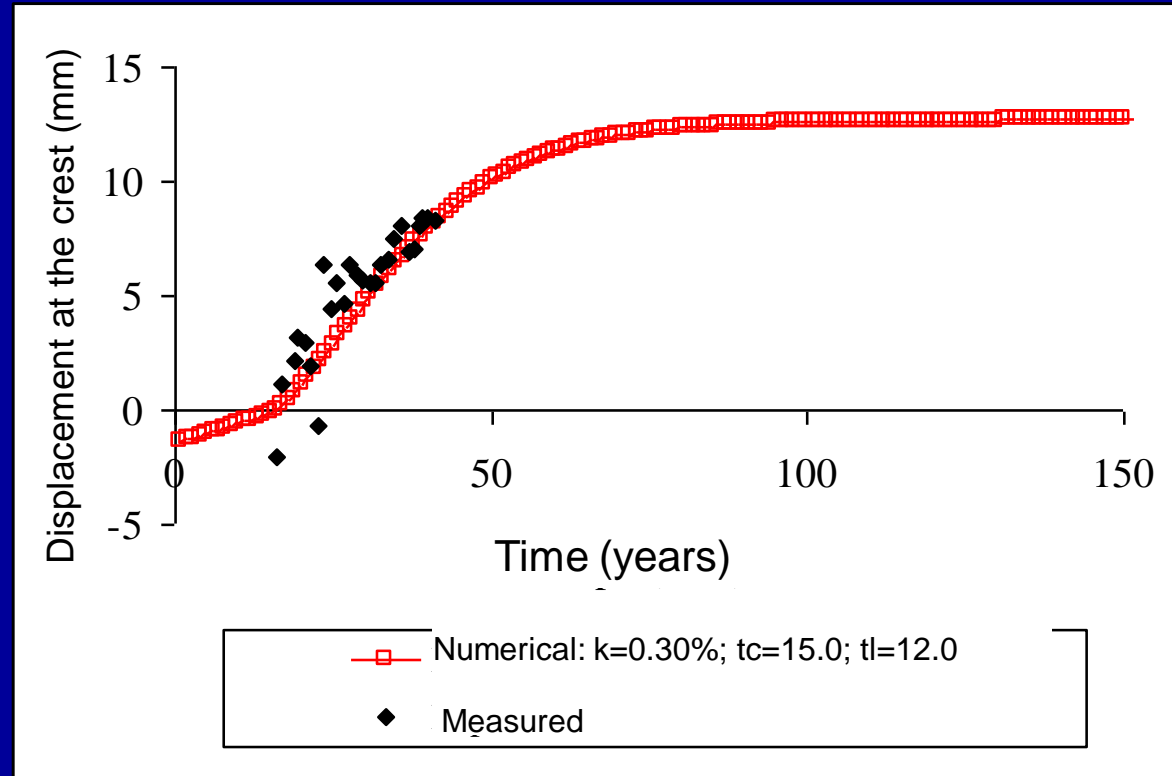
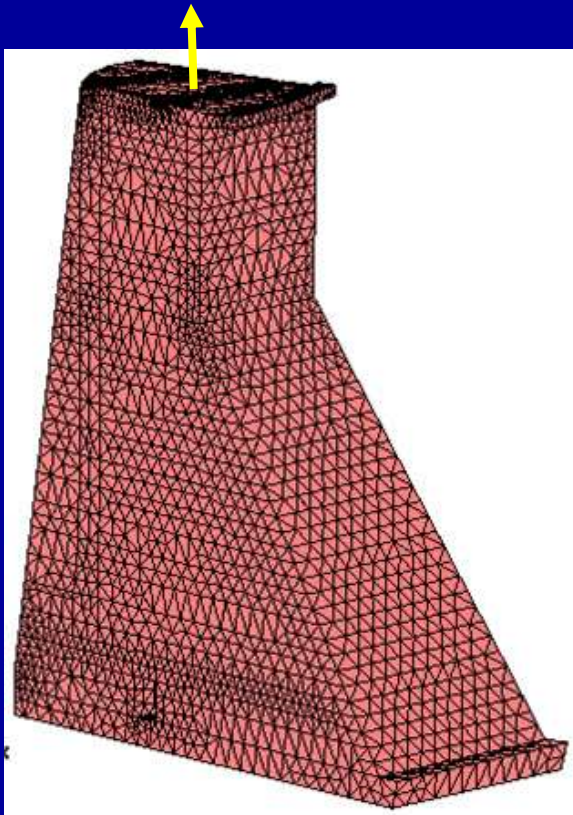
Furnas dam: moisture fields – averaged steady state



Furnas dam: displacements at the crest



Furnas dam: displacements at the crest



Concluding remarks

- Model thermo-hygro-chemo-mechanical with stress-induced anisotropy:

Can simulate the evolution of the chemical reaction and of its mechanical effects, considering temperature, moisture and cracking effects on the evolution of swelling.

- Numerical modeling (Finite Element Method):

3D operational FEM computer code allows for the execution of real analysis on complex geometries with a large number of degree of freedom. It is then possible to predict the evolution of the effects of the reaction.

- Inverse analysis (experimental and numerical):

Allows for the identification of parameters – structural or local levels.

Acknowledgements



FURNAS – CENTRAIS ELÉTRICAS
S.A.



FIM